



Preliminary Fracture Analysis
of Þeistareykir Geothermal Field
and Surroundings, Northern Rift Zone
and Tjörnes Fracture Zone

Preliminary Fracture Analysis
of Þeistareykir Geothermal Field
and Surroundings, Northern Rift Zone
and Tjörnes Fracture Zone



ÍSOR-2013/029

Project no.: 13-0212

December 2013

Key Page

LV report no: LV-2013-116 **Date:** December 2013

Number of pages: 57 and 2 maps **Copies:** 12 **Distribution:** On www.lv.is
 Open
 Limited until

Title: Preliminary Fracture Analysis of Þeistareykir Geothermal Field and Surroundings, Northern Rift Zone and Tjörnes Fracture Zone.

Authors/Company: Maryam Khodayar and Sveinbjörn Björnsson

Project manager: Ásgrímur Guðmundsson (LV) Anette K. Mortensen and Magnús Ólafsson (ÍSOR)

Prepared for: Prepared by Iceland GeoSurvey (ÍSOR) for Landsvirkjun.

Co operators: _____

Abstract:

We extracted the fracture pattern of Þeistareykir from eight versions of spots, orthomaps, and aerial photographs to obtain a more comprehensive view of rifting and transform faulting. In an area of roughly 170 km² covering the Þeistareykir geothermal field and its immediate surroundings, we identified 10729 old and young fracture segments in Late Quaternary-present series that includes Miocene, locally. The total number of structures is, however, less as single fractures consist of several segments along traces. The structures are faults, open fractures and prominent joints. Their structural analysis shows that: (a) Four sets striking northerly, ENE, WNW and NNW emerge from statistical analysis of the data. Two additional sets, NNE and E-W are also visible on the maps. These six sets control to a large extent the tectonic, morphology, lava structures, eruptive cones, and influence the geothermal activity. (b) All sets have dip-slip component, ranging overall from 0.5 m to more than 200 m. The largest slips are on rift-parallel northerly normal faults then on the NNW set in the bedrock. (c) The en échelon arrangements of fractures indicate sinistral motion on NNE to ENE sets, and dextral motion on WNW to NW sets. Regional focal mechanisms and relocated earthquakes show the same strikes and motions. (d) Open fractures strike mostly northerly, NNE and NW, less WNW and ENE, and almost none is E-W. (e) Northerly, WNW and ENE fractures are the most frequent, while E-W set is the least common and has the shortest segments. The northerly rift-parallel fractures constitute 1/3 of the total fracture population. (f) Geometrically, all but the E-W set are regularly distributed in the area in parallel weak zones of major or minor fractures. The trace of the Húsavík Fault is straight and differs from the NW fractures. Pronounced sinuosity in single structures results from intersecting fractures of various strikes, which will have different motions under the stress field. (g) In the centre of the Þeistareykir fissure swarm there are two young northerly grabens separated by a ~ 2 km wide WNW fractured zone, which contains a WNW ridge. Likely, the last postglacial eruption occurred on this WNW dextral segment at Stórhver crater at the summit of the ridge. (h) The well ÞG-8 intended to intersect northerly fractures and an eruptive fissure at Stórhver. But it is unlikely that the major boundary faults of the grabens intersect this crater. We identified a few major fractures forming “fracture zones” or “weak tectonic zones” intersecting the well as being mostly of transform character. A simplified correlation indicates that our suggested fractures coincide with three reported aquifers in the well. (i) The correlation with well and earthquake data shows that the suggested fracture sets in our study are of tectonic origin. These fractures have been reactivated through time, controlling the permeability at depth. Our results bring new insights into the tectonic of Þeistareykir, but more correlation with and structural analysis of subsurface data is required before the results can be used for well siting.

Keywords:

Þeistareykir; Geothermal activity; Tectonics; Fracture permeability; Northern Rift Zone; Tjörnes Fracture Zone

ISBN no:**Approved by Landsvirkjun's
project manager**

Project manager's signature 	Reviewed by  ÓGF
--	---

Table of contents

1	Introduction.....	7
2	Geological context.....	8
3	Methodology	10
	3.1 General consideration.....	10
	3.2 The applied method.....	10
4	Analysis of the fracture population.....	12
	4.1 Main features of the fracture pattern.....	13
	4.2 Lava structures and eruptive craters.....	15
	4.3 Surface alteration.....	16
5	Interpretation	16
6	Brief correlation with earthquake and borehole data	20
	6.1 Earthquake data	20
	6.2 Well ÞG-8 as an example.....	21
	6.2.1 Well data	21
	6.2.2 Televiewer data.....	23
7	Summary	25
8	Recommendations.....	27
9	References.....	28
	Annex to the methodology and use of aerial imageries.....	32

List of tables

Table 1.	<i>Image types used in this study and their features.</i>	11
----------	---	----

List of figures

Figure 1.	<i>The outline of the area covered by observations of aerial imageries in this study and location of boreholes at and surrounding Þeistareykir.</i>	36
Figure 2.	<i>Compilation of tectonic elements of rift and transform zones plate boundaries in North Iceland.</i>	37
Figure 3.	<i>Overview of geological and geophysical studies.</i>	38
Figure 4.	<i>Examples of image types used in this study and their coverage on the ground.</i>	39
Figure 5.	<i>Examples of how structures appear on each image type.</i>	40
Figure 6.	<i>Map showing the type of image used to draw the fracture pattern.</i>	41
Figure 7.	<i>Statistical analysis of the fracture population</i>	42

Figure 8. <i>Schematic block diagram made for this study to show possible fracture geometries, their surface expressions, and the resulting horts and grabens</i>	43
Figure 9. <i>Examples of fractures (1)</i>	44
Figure 9. (Cont.) <i>Examples of fractures (2)</i>	44
Figure 10. <i>Examples of dextral strike-slips based on the left-stepping en échelon arrangement of open fractures.</i>	46
Figure 11. <i>Examples of sinistral strike-slips based on right-stepping en échelon arrangement of open fractures at the surface.</i>	47
Figure 12. <i>Highlights of rift-parallel northerly fractures / weak zones in Þeistareykir fissure swarm.</i>	48
Figure 13. <i>Highlights of NNE / NE fractures / weak zones.</i>	49
Figure 14. <i>Highlights of ENE fractures / weak zones.</i>	50
Figure 15. <i>Highlights of E-W fractures / weak zones.</i>	51
Figure 16. <i>Highlights of WNW fractures / weak zones parallel to the transform zone of Tjörnes Fracture Zone.</i>	52
Figure 17. <i>Highlights of NW fractures / weak zones.</i>	53
Figure 18. <i>Summary interpretation of the most significant fractures / weak zones and their motions. Note that the lines here do not represent single fractures.</i>	54
Figure 19. <i>Correlation of our fracture pattern with relocated earthquakes (M -0.6 to 3.2) from 1993 to 2011.</i>	55
Figure 20. <i>Brief correlation of our fractures with data from well ÞG-8.</i>	56
Figure 21. <i>Fractures and widest broken zones from televiewer data along with circulation losses in well ÞG-8.</i>	57

1 Introduction

Landsvirkjun has interests in the geothermal fields of North Iceland. Due to their locations near or at rift and transform plate boundaries, these fields are fracture-controlled. Thus changes in the reservoirs or even the presence and location of the fields themselves are dominated by tectonics. Although crustal movements and earthquakes have been monitored at or around these fields continuously, a standard structural analysis has not been carried out for the past three decades to include the picture of tectonic beyond present-day deformation.

Peistareykir is chosen as an example for such a structural analysis. The field is within the Northern Rift Zone (NRZ) and Tjörnes Fracture Zone (TFZ), undergoing complex deformation resulting from both rifting and transform faulting. Several wells have been drilled in this field on the ground of previous geological and geophysical studies with varied success (Fig. 1).

In order to better tap the geothermal resources a comprehensive map that reflects the fracturing of both the rift and the transform zone is needed. Such a thorough map is not at hand as intensive geological and geophysical studies dealt mostly separately with the tectonic of the rift and the transform zone. The present study offers a much-needed structural analysis of this field, which could help to understand better how the tectonics of both plate boundaries affect the geothermal activity and thus define drilling targets. The first step of such a study is to update the fracture population of the Peistareykir field and surroundings since the work of Gíslason et al. (1984). The purpose of this report is twofold:

- Prepare a new map of the tectonic pattern of NRZ and TFZ at Peistareykir from aerial imageries along with a structural interpretation of the fracture population.
- Brief correlation of the results with faults indicated by earthquakes and selected borehole data from well ÞG-8.

It is important to bear in mind that such a structural analysis cannot start from the field because: (a) To cover a representative portion of the land reflecting rifting and transform faulting would require several field campaigns and large manpower, and the results would not be available until after many years. (b) A part of the structures is subtle without major prominent traces. They could easily be blended with the structures of the younger lavas in the field, but they are well visible on aerial imageries. **Field studies, however, should follow this work based on imageries to check and collect more data.**

As most of the exposures around Peistareykir are poor, mapping of the fractures in an area limited to Peistareykir itself and expanding from there would not yield an understanding of the overall influence of rift and transform zones. A larger representative area is required. Therefore, we made an effort to cover a representative portion of the land within a frame of roughly 170 km² (Fig. 1), similar to that used by Gíslason et al. (1984). In addition to new observations and interpretation, we offer the basic data in GIS for further use.

Results of our preliminary work here offer insights into the tectonics of Þeistareykir, but require more correlation with, and structural analysis of subsurface data, along with field studies, before results can be used for well siting or in other projects.

2 Geological context

Due to its location at the junction of NRZ and TFZ (Fig. 2), Þeistareykir geothermal field undergoes deformation from both types of plate boundaries. The tectonic history here is complex, spanning several million years and including plate reorganisations, flexuring, intense fracturing, and rotation. Very briefly: (a) An early rift segment was active at Húnaflói-Skagi from 9.5 to 13 Ma, and emitted flood basalts as well as some acidic rocks (Jancin et al., 1985). Bedrocks from this period are found as far as north of our study area. About 6–7 Ma, the rift shifted some 130 km eastwards to the present NRZ, and the new spreading centre also emitted flood basalt along with acidic rocks and hyaloclastites. An unconformity separates the series of the two rifts. In general, synclines form at the active rifts due to tilt and extension (Pálmason, 1980), and as a response, “anticlines” form between the two spreading centres. The younger lavas, therefore, deposited on the flank of an older flexure dipping 15°–35° SE. The transform zone of TFZ connected the spreading centres and has been active at least since 7 Ma. The dextral displacement on TFZ is considered 100 km (Sæmundsson, 1974; 1978) to maximum 140 km (Jancin et al., 1985). However, the shift of the rifts occurred via several short-lived spreading centres, one of which could have been the Skagafjörður paleo-rift, which was active 6–3 Ma (Garcia et al., 2003). It is also speculated that the TFZ has had a longer lifetime (Young et al., 1985; Jancin et al., 1985). A progressive rotation of lavas, 0°–110° clockwise, is reported from Flateyjarskagi along with rotation of dykes and faults very near the TFZ. Northerly faults are considered purely extensional, while a system of Riedel shear is suggested from the analysis of the fracture pattern of the older crust (Voight and Mamula, 1983). Both the TFZ and the Riedel shears have an oblique character, i.e., a combination of dip and strike-slips. Mineralisation in the fractures of the older crust indicates that both rift and transform systems controlled the geothermal activity in time and depth (Young et al., 1985).

Þeistareykir geothermal field is more precisely at the junction of Þeistareykir-Mánáreyjar fissure swarm (i.e., the westernmost swarm of NRZ), half of Mánáreyjar swarm being offshore. The field is also between the Húsavík Fault and the Dalvík lineament (Fig. 2). A closer look at the details of these plate boundaries is essential to understand the local geological context.

- The series found in Þeistareykir-Mánáreyjar swarms are: (a) Miocene to interglacial and sub-glacial (Brunhes-Weichselian) series consist of lavas and hyaloclastites, with local rhyolite at Mælifell to the northwest of Þeistareykir, as well as andesite and dacite. Contrary to Krafla fissure swarm, no apparent volcanic centre stands out in Þeistareykir and acidic rocks are insignificant at the surface. Marine fossil-rich sediments deposited unconformably during Pliocene (Tjörnes beds) and Quaternary (Breiðavík beds) mostly West of Mánáreyjar swarm near the northern shores. The northern part of our study area covers a very small portion of the regional unconformity. (b) Postglacial lavas are younger than 15,000 yrs and the last eruption of Þeistareykir swarm occurred 2600 yrs. ago (Þeistareykjahraun lava) with picrites emitted from the Stórhver crater

(Sæmundsson et al., 2012a). In the Krafla swarm, magma injection into dyke is thought to be responsible for the 1976 Kópasker earthquake (Björnsson et al., 1977; Brandsdóttir and Einarsson, 1979) (Fig. 2). The last eruption of Mánáreyjar occurred in the unrest period of 1868–1885 (Sæmundsson et al., 2012a) that included large earthquakes on the HF and in Öxarfjörður (Thoroddsen, 1899).

- The TFZ is some 120 km long and ~ 70 km wide and connects the NRZ to Kolbeinsey ridge offshore north Iceland. The rate of spreading along these rift segments is 1.8 to 2 cm per year in the direction of N105° (Geirsson et al., 2010; DeMets et al., 2010). (a) Within the 70 km width, the TFZ consists of three major WNW trending structures: Grímsey, Húsavík-Flatey Fault (HF), and Dalvík (Fig. 2). Only the HF presents an established fault plane in the outcrop showing dextral motion, confirmed by earthquakes offshore on the fault plane itself (Rögnvaldsson et al., 1998). The Grímsey lineament is not a defined fault plane but an oblique zone (Grímsey Oblique Rift-GOR) similar to the oblique rifting in Reykjanes Peninsula (Einarsson, 1991). Here, dextral motion of this zone is taken up by sinistral motion on shorter NNE strike-slip faults (e.g., Rögnvaldsson et al., 1998). Presently, the HF is locked and the GOR takes up to 60% of the deformation in the TFZ (Metzger et al., 2011). As to Dalvík lineament, while the lineament has a sharp signature in the topography in its eastern part, earthquakes are recorded mostly in the western part of this structure on northeasterly sinistral strike-slips to the north of the lineament (Stefánsson et al., 2008). (b) GPS measurements indicate continuous deformation associated with TFZ, with earthquakes up to M7 (Einarsson and Björnsson, 1979). One or two earthquakes >M6 have occurred on each of the three transform lineaments in the last three centuries.
- Focal mechanisms of earthquakes in the TFZ indicate strike-slip motions on northerly/northeasterly, NE, WNW and NW fracture segments (Rögnvaldsson et al., 1998), supported by relocated earthquakes at Þeistareykir (Hjaltadóttir and Vogfjörð, 2011). A number of works both in the adjacent old crust of Flateyjarskagi (Voight and Mamula, 1983; Young et al., 1985), and in the younger series of Þeistareykir (Gíslason et al., 1984) also show existence of these fractures typical of transform faulting. On geological maps (Fig. 3a), the fracture pattern of Þeistareykir and surroundings favours northerly normal faults and fissures parallel to the rift and a few WNW segments (e.g., Sæmundsson et al., 2012b).
- The exploration of Þeistareykir geothermal field has included geological mapping (Fig. 3a); resistivity (Fig. 3b); surface alteration; water geochemistry, and gas geothermometry; (Sæmundsson, 2007; Gíslason et al., 1984; Karlsdóttir et al., 2012; Kristinsson et al., 2013; Óskarsson, 2011). A number of shallow exploratory (ÞR-1 to ÞR-11; and ÞP-2 to ÞP-4 and ÞP-6), and deep exploration wells (ÞG-1 to ÞG-9) have been drilled up to now (Fig. 1). The deep wells have generally a satisfactory output, except well ÞG-8 (e.g., Mortensen, 2012).

3 Methodology

3.1 General consideration

Observations of aerial imageries offer great possibility to extract information on the bedrock and tectonics. The method is time consuming particularly when different types of images are used or the study area is large, requiring careful inspection and trained eyes. It is, therefore, necessary to clarify the value and difficulties of the method, not the least what one might obtain from it compared to geological mapping solely done in the field. This we do in great detail in the accompanying document labeled as **Annex**. To prevent misunderstanding, we define here how we use a few terms:

- A “fracture” can be a normal fault, a strike-slip fault, a prominent joint, or a dyke even though dykes are rare in the study area. A clarification is needed for the use of the terms “**fractures**” and “**lineaments**”. These terms are used internationally in a very flexible manner without one term referring to a specific origin and the other term to another origin. Accordingly, in this study we use these two terms alternatively as fits the sentences. When we are not sure about a fracture trace or have doubt about its tectonic origin, we have labeled it as “possible” on our maps and figures (for further discussions about the likeliness of non-tectonic origin of fractures see Annex).
- The term “dip-slip” refers to a fault with normal component, i.e., the case of pure normal faults. Some of the strike-slip faults in this extensional context have also a normal component, in which case they are oblique-slips. Pure strike-slips do not have a dip-slip (normal component in this extensional context) and the motions are horizontal shears along the strike of the faults. In rare cases where we identified strike-slip motions, they also have normal component (dip-slip), in which case they are in reality oblique-slip faults.
- “Undifferentiated” refers to definite fracture traces where it cannot be determined from aerial images if the structure is a dyke (rare at the surface in this area due to shallow erosion), a fault or a joint. In some cases the structure is clearly a fault, but whether the lineament is a pure normal fault, a strike-slip fault or an oblique-slip fault cannot be identified due to the image resolution. “Possible” fractures are those where a lineament of tectonic origin is well visible in the landscape on the images, but its exact trace cannot be determined due factors such as the image quality, or erosion that blurs the sharpness of the fracture plane. **Often segments marked as “possible” on the maps fall along the traces of major longer fractures/faults.** Faults with “dip-slip” (normal component) are those where the downthrown blocks could easily be identified. Faults with “possible dip-slip” have visible vertical displacements in the landscape but the sense in which the block is downthrown cannot be clearly defined.

3.2 The applied method

To reduce the cost of this work, it was decided to restrict the survey to the in-house spots, orthomaps, and aerial photographs available at the time of this study. Figure 4 shows an example of each type of images and their coverage. On these images, the structures appear

due to contrasts between light and shadow. As the images have been taken at different heights and angles, each type offers a different depth for observation.

Spot images cover the entire study area. This type of image has more depth and is more suitable for the overall fracture trace and regionally. The color and black & white orthomaps from 1998 cover a part of the area diagonally. Those from 2007 have less coverage, but they do cover locally areas that cannot be seen on the 1998 images (Fig. 4). Due to their resolution, orthomaps are best for more detailed information and near observations of the structures. Available aerial photographs in-house cover most of the study area but do not reach south and east of Bæjarfjall. These photos are suitable for both relative regional and local observations.

The spot and orthomaps images are corrected so that when drawing a feature in GIS on top of these images, the drawing is with coordinates and without distortion. The draw-back with this type of images is that they do not offer the possibility of observing in stereo (relief). Aerial photographs, on the other hand, offer possibility of observations in relief, but the process requires pairs of photos, stereo, and trained eyes. Regardless of the year they were taken, aerial photographs are by far the best type of images. However, due to distortion in the location of structures on this type of images, observations cannot be done directly in GIS, but first on aerial photographs then reported manually onto other image types in GIS. Because of this time-consuming process, aerial photographs were used only when it was necessary to check the fracture trace or the dip direction of a fault.

As the interpretation of fractures relies much on the quality and scale of the images, in reality 8 versions of images were used in this study (Table 1):

Table 1. *Image types used in this study and their features.*

Image type	Color	Year	Resolution on the ground
Spot	Monochrom	2003	2.5 m (per pixel)
Spot	Composite	2003	2.5 m (per pixel)
Spot	Infrared	2003	2.5 m (per pixel)
Orthomap	Color	1998	0.5 m (per pixel)
Orthomap	Black & White	1998	0.5 m (per pixel)
Orthomap	Color	2007	0.5 m (per pixel)
Orthomap	Black & White	2007	0.5 m (per pixel)
Aerial photographs	Black & White	1960 and 1961	30 m (per mm)

Figure 5a shows the easiness of observations in the study area, which is mostly function of the rock type and altitude of exposures. The older hyaloclastites mountains are topographically high and observations are marked “easier” there on the images. The younger (postglacial) lavas < 15.000 years occupy the low-land. There, observations are less easy in the central part of the study area and difficult (marked least easy on Fig. 5a) in the eastern part, particularly to the north of Bæjarfjall. The reason for this is the poor exposure. Except for open fractures, the traces of other young fractures are subtle. This is partly because the displacements of younger faults do not create major variations in the topography

for prominent light/shadow variations, and partly because the subtle traces of fractures can be blended with, and mistaken for the structures of the postglacial lavas. When using the fracture maps from this study, it is important to bear in mind the following:

- Seeing a fracture depends much on the scale and the light. A fracture may not be visible in a “zoom-in” mode, but prominent on a “zoom-out”. The traces and strikes of a fracture can be slightly or much different on images, be it within the group of spots images, orthomaps and aerial photographs, or between image types (Figs. 5b to 5g). Figures 5h and 5i show a close-up of an example of these differences.
- Considerable efforts were made to prepare a complete picture of the tectonic pattern by extracting as much as possible the fractures - in the rock. To this effect, fractures were first observed on the ground of spot images at different scales. Then their traces were rechecked / completed / modified with various orthomaps and aerial photographs. To deal with the issue of lava structures, we also mapped as many lava tubes and lava channels as possible to exclude them from the lineament map (Map 1). Figure 6 shows on what image type the final drawing of a fracture trace was made.
- The total fracture population presented in this study cannot be extracted from one image type alone as a single fracture trace may be visible only on one type of image but not on the others. Thus the proposed maps are the result of combined observations of the 8 versions of imageries.
- Preparing the fracture maps from aerial imageries in this study benefits from our similar experience in other areas of Iceland where Tertiary to present rift and transform faulting co-exist, namely in West (Khodayar et al., 2004) and South Iceland (Khodayar and Einarsson, 2006; Khodayar, 2013). Those studies in turn benefitted from intensive field work (e.g., Khodayar, 2009; Khodayar et al, 2011; Khodayar and Björnsson, 2013) where the structures from aerial images could be checked during outcrop mapping.
- Our study of Þeistareykir is the first attempt to interpret the fracture population of this area using a methodology we used efficiently elsewhere. Although our methodology and results offer new insights, a second phase of work is required to correct some of the uncertainties by using better quality images, locally, and by carrying out field work as commonly done in similar studies cited above.

4 Analysis of the fracture population

A total of 10729 fracture segments were identified from aerial imageries (Fig. 7) and presented in various figures and maps in this report. Maps 1 and 2 show all geological features interpreted for the purpose of this study along with the overall tectonic pattern. For reference, these are reported on a topographic (Map 1), and image (Map 2) supports.

Four geological features were selected for interpretation: (a) We simplified the groups of relative rock ages suggested by Sæmundsson et al. (2012b) to two: Older bedrock (Miocene-Late Quaternary) and younger lavas (postglacial lavas younger than 15.000 yrs). We also identified a great number of lava tubes and lava channels to distinguish them from possible fractures. (b) Surface geothermal alteration as observed in this study. (c) Pleistocene and

postglacial craters interpreted by us. (d) Fracture population, distinguished in terms of its relative age (younger and older), and types (open fractures, normal faults, and undifferentiated fractures).

4.1 Main features of the fracture pattern

- *Fracture trace and geometry.* The length of the mapped segments ranges from 4.5 m for the shortest, to 2217 m for the longest. These segments have, however, different weights (Fig. 8). Their traces are more or less easy to detect on images ranging from sharp (Figs. 9a and b) to less prominent (Figs. 9c and d) and even to subtle particularly in the youngest Þeistareykjahraun lava (Fig. 9e). Major fractures have either longer traces or a more prominent signature in the topography. Minor fractures are either shorter in length, or their slip has not lead to significant changes in the topography. Those lineaments marked as faint/gashes are even less prominent partly because of the quality of images and partly because the surface expressions are not so obvious or the fractures have not been subject to major/repetitive deformation. Possible fractures are breaks in the ground where either their exact trace or their existence cannot be confirmed due to poor exposure or the quality of the image. It is important to note that a segment may be called minor locally due to its discrete trace although it could be a part of a major and longer fracture. Figure 8 gives a few examples of the possible geometries discussed above. Most identified fractures have a straight trace especially when they are shorter. But on a map, fracture traces may present gentle sinuosity, which affects the local strike of the fracture by a few degrees but not its overall trend. Finally, a number of longer fractures display a “V” shape geometry (Maps 1 and 2), which results from one fracture joining another and continuing as a single segment.
- *Fracture frequency.* As a very first step, a preliminary statistical analysis of the fracture population in the entire area is prepared to find out the most frequent strikes (Figs. 7b and 7c) although much more statistical analysis is needed at a later stage. It is strongly emphasised that **10729 is not the total number of faults cutting the rocks as a single fracture or fault often consists of several shorter segments along its trace** (Figs. 7a, 8, and Map 1). An attempt to prepare a rose diagram using directly the strike of individual segment (10729) and the strikes of individual segment did not deliver a convincing result as a very short segment was counted in the same manner as a long major segment. Therefore, we attempted another method in which the frequency of the strikes is shown on the basis of the length of individual segments. Very simply explained, the strike of a segment with a length of, for example, 100 m appears in the statistics 10 times more than the strike of a segment with a length of 10 m. The results are shown in detail a diagram with a 1° interval in the strikes (Fig. 7b) and again in a rose diagram with 10° interval for a standard reading (Fig. 7c). Figure 7c in particular, shows clearly that the northerly fractures (N0°–N20°E) with a peak at N11°–20°E are the most prominent. Equally common are the WNW (N111°–130°E) fractures with a peak at N121°–130°E, and the ENE fractures (N51°–70°E) peaking at N61°–70°E. On Fig. 7b, the NW fractures (N151°–170°E) have a strong peak at N151°E, while on both Figs. 7b and 7c the NNE fractures (N21°–30°E) are less common and the E-W ones (N81°–90°) the least frequent of all fractures. These results are concordant with the visual assessment of the fractures on the maps. Three important features stem from these diagrams: (a) If the fracture identified from

aerial images here were not of tectonic origin, then they would most likely appear either with random strike distributions or in equal amplitude in all directions. But both diagrams show that there are preferred strikes. A fracture pattern with such organised sets cannot be but of tectonic origin and a response to the regional stress orientation. (b) The two most common fracture sets, i.e., northerly and WNW, are respectively those of the NRZ fissure swarm (mostly N5°–15°E) and TFZ (mostly N115°–125°E). (b) As the table in figure 7c shows, the most important result of this statistical analysis is that the northerly fractures of the rift fissure swarms (N0°–20°E) constitute only 16.5% of the total length of the fracture population. A similar result was obtained from the analysis of large fracture populations in West Iceland (Khodayar et al., 2004) and in South Iceland (Khodayar et al., 2011), as well as a smaller population in Húsmúli (Khodayar, 2013). Without entering the mechanism of unstable plate boundaries, the feature common to all of these areas is their locations within both the rift and transform zones, regardless of whether they are extinct or presently active. Further statistical analysis is needed to fully understand the fracture pattern of Þeistareykir.

- *Fracture types.* Dykes are not observable in the study area because the level of erosion in the older and younger rocks here is not sufficient to expose these structures. Only in two places co-workers have observed in the field few shallow thin dykes in the hyaloclastites. One is north of Lambahnjúkur (Sæmundsson et al., 2012a), and the other in Ketilfjall (Sæmundsson, 2007), respectively to the west and east of the study area. As these dykes are too thin to be identified on aerial images, we reported their traces on our maps as suggested in the works of the above authors. Consequently, the fractures analysed in this study are faults, open fractures, and prominent joints (see the definitions of undifferentiated and possible fractures in chapter 3.1).

As defined earlier, faults with dip-slips are those, which could be definitely identified on the basis of the downthrown blocks. Open fractures are all young with apertures up to 2–3 m as judged from aerial imageries (Figs. 9, 10, and 11). All faults have dip-slip component regardless of their strikes (Figs. 9a to 9e). The magnitude of vertical displacements is less along minor or younger faults and more along older major faults (Fig. 9a), i.e., 0.5 m to 200–300 m, respectively. The highest dip-slips are along northerly faults. This is not surprising given that regional spreading in the direction of N 105° (DeMets et al., 2010) takes place in North Iceland primarily on northerly fractures of the rift fissure swarms. Strike-slip motions, on the other hand, are more difficult to identify on aerial imageries (and in the field) partly because their small horizontal offsets do not create major changes in the topography, and partly because the resolution of the images is not enough to see such subtle displacements. Based on their en échelon segmentations, however, we identified few possible strike-slips along several fracture sets, but overall, fractures displaying such obvious arrangements are not common here. The left-stepping arrangements typical of dextral motion were observed along the WNW set (Fig. 10a), i.e., fractures parallel to TFZ. A second possible set with dextral motion could be the NW (Figs. 10b and 10c). The right-stepping en échelon arrangement was observed along the NE fractures (Figs. 11a to 11c), more precisely NNE to ENE.

Three important features are to be retained. (a) When exposures are enough on aerial imageries, fracture planes seem to be steeply dipping, estimated as $\geq 75^\circ$. (b) Parallel fractures with dip-slip dipping towards each other form grabens (of any size) and those

dipping away from each other control horsts (Fig. 8). (c) In many cases, individual fractures appear on maps dipping towards one direction along one segment and towards the opposite direction along another segment, which is possible only when faults are steeply-dipping such as in Iceland.

- *Relative age and reactivation.* Fractures cannot be dated absolutely. However, we made an attempt to group them in terms of old and young as best as possible (Map 1). This distinction was done on the ground of the surface expression of the fractures and the age of the rock they were observed in. Older fractures are with distinct topographical expression. They are usually higher up in the altitude and display the hyaloclastites and lavas older than 15.000 yrs. Younger fractures are for the majority in the low land and cut the lavas younger than 15.000 yrs. But a few young fractures could be identified in the older series as well. Younger fractures consist of shorter segments with fresher traces, particularly the open fractures. As most of the study area is covered by the younger lavas, a great portion of the fracture population is marked as young on our maps. However, close inspection of the structures shows that all sets of fractures are reactivated. This is visible in the western or northern parts of the study area. From there the traces of older fractures with prominent dip-slip continue into the younger lavas where the segments have much less or no slips, or appear just as open fractures. This observation points to fracture reactivation or a continuous deformation where the upper crust breaks along the same weakened strikes and zones.

4.2 Lava structures and eruptive craters

Although evidence of glacial erosion and deposition is recorded nearby to the west and east of Þeistareykir, the lavas younger than 15.000 yrs in the study area do not seem to have been subjected to glacial processes (Sæmundsson et al., 2012b). Therefore, these fresh lavas have kept most of their surface or flow structures, some of which can easily be mistaken for fractures. Therefore, we mapped as much as possible the lava tubes and lava channels (Map 1), to distinguish these lava structures from subtle tectonic lineaments in the youngest 2600 yrs postglacial lava. Lava channels are distinct structures with a width in order of few metres maximum and lengths that can reach tens of metres. They can be short and straight, or long and sinuous. Lava tubes are small crater-shaped structures, and very shallow in depth, aligning in rows. They too can be straight or sinuous. Regardless of their dimensions, the edges of the lava channels or the overall traces of lava tubes sometimes coincide, subtly or strongly, with fractures. This indicates continuous deformation and fracturing even during magmatic eruptions, lava flows and consolidation.

It has been discussed if mapping of lineaments as indication of fractures can at all be justified in postglacial lavas unless the fractures are quite obvious in the field. Annex discusses thoroughly the fracturing and ages, but three arguments should be mentioned here that are supportive of the presence of fractures in the postglacial lavas: (a) Postglacial lavas span the last 15.000 yrs. (Sæmundsson et al., 2012a). In these lavas, prominent northerly fractures of the rift are favoured on maps even if there are also obvious but more subtle northerly fractures, which traces cannot be easily seen identified in the field. There are also fractures of other directions, i.e., WMW for example (Gíslason et al., 1984). Our own observations here support the mapping by Gíslason et al. (1984), and complete the pattern with a few additional fracture sets, with obvious examples in the postglacial lavas shown on Figs. 9 to 11.

(b) Favours northerly fractures because they are more obvious may lead to a misleading interpretation that the TFZ has not been active over the past 15.000 yrs and it did not create major or minor fractures in those lavas. This is incorrect because TFZ has been active over the last 7 Ma years in the same position as is today, and the frequency of major earthquakes (M 6–7) within it is about 2 per centuries in the area of postglacial lavas. However, we have already pointed out that mapping the more subtle fractures of any direction may be difficult for untrained eyes, or if the idea is that the rift has been the sole active mechanism in the area over the last 15.000 yrs. (c) We have specifically inspected the distribution of “lineaments” in postglacial lavas of various ages. Not only we found that the pattern there show statistically significant preferred directions that are similar to what is found outside the youngest postglacial lavas, but in most cases the subtle fractures in the 2600 yrs lava extend along the same exact strike into the older postglacial lavas and even into the bedrock. Therefore we are comfortable with using the “lineament” study also in the postglacial lavas.

Many eruptive craters were observed on the images. Due to the resolution of the images, their number is higher than on the geological map of North Iceland (Sæmundsson et al., 2012b). We grouped the mapped craters into the same categories of postglacial and Pleistocene as on the geological map of North Iceland. In our observations, we notice that postglacial craters are much smaller in diameter, from 5 m to tens of metres. They are fresh and generally round in shape, except for Stórhver, which is elongated mostly WNW. Pleistocene craters are much larger and are circular or semi-circular. They are mostly in Bæjarfjall and surroundings and reach ~ 850 m in diameter. Regardless of their size and shapes, the eruptive craters are almost always aligned on fractures, whether on a single one or at the intersection of several sets.

4.3 Surface alteration

The alteration was mapped on the ground of various image types, but mostly orthomaps. This means that the mapped contours represent the status of alteration until 2007, i.e., the year of the newest orthomaps used. We grouped the alterations into three categories based on visual inspections of their colors and textures on the images (Map 1). One group presents definitely the characteristics of advanced geothermal alteration and appears as strong white continuous patches on images. The second category is also white, but more subtle and dispersed. The third category is sparse and darker, similar to clay or subtle early-stage alteration. Because these features are mapped from aerial images, the two latest categories with subtle appearance are labelled as “possible”.

Note that the alteration suggested by Gíslason et al. (1984) in the western part of the study area to the southwest of Mælifell is not visible on the images.

5 Interpretation

The following interpretation of the fracture pattern is preliminary as time was mostly spent in extracting the fractures from aerial imageries. We interpret the fracture pattern in terms of “main important” or “weak zones” along with their likely motions to give an overview of the tectonic context in which Þeistareykir geothermal field is located. It is important to recall that a fracture consists of several segments along its trace. These segments may be locally minor

or major, or tightly parallel, forming a prominent fracture or a deformation zone (called also weak zones). Beside their traces, we used other features such as morphostructural signatures of the segments in the landscape, pronounced trace or displacement, control of lava structures by fractures, etc., to highlight the most important weak zones.

Figures 12 to 17 present each of the 6 fracture sets separately. We highlighted on each of the maps the most important structures that we estimate being the weakest zones. The interpretation of the fracture pattern shows several interesting features:

- The Þeistareykir fissure swarm consists of old and young northerly normal faults as well as young open fractures (Fig. 12; Map 1), spread within a roughly 9 km wide area coinciding with the definition of this fissure swarm by Sæmundsson et al. (2012a). We see the western boundary of the swarm to be roughly where the postglacial lava and eruptive cone are on a young northerly fault to the north of Skessuskál (Map 1). The boundary of the swarm to the east is at or very near Ketilfjall although this hill has been interpreted as a hyaloclastite ridge in previous studies and not as a weak tectonic zone. The trace of this structure is sharp on spot images, possibly dipping to the west, indicating a normal fault zone that controlled the older hyaloclastites ridge and had recent activity (Map 1). Farther south, the eastern boundary of the fissure swarm could be the easternmost open fractures going through Kvíhólafljöll (Map 1). This boundary to the south is thus slightly shifted to the east compared to Ketilfjall. The fractures to the south and southwest of Bæjarfjall are a blend of open fractures and very small-scale normal faults whose dip-directions are very difficult to determine on images. Interpreting a subtle structure as a normal fault or an open fracture, however, affects how the geometry of major structures such as a graben is determined within the fissure swarm itself. In our study, we see in the northern part a young graben filled by the 2600 yrs. Þeistareykjahraun, rather to the mid-west of the fissure swarm. The graben is sharply bounded along three of its flanks with the following faults: (a) The WNW Húsavík Fault at Sæluhúsveggur to the north, dipping to the southwest, and with a dextral strike-slip motion. (b) To the west, the northerly open fractures and small-scale normal faults of Litla-Mælifell dipping to the east; (c) To the east, same type of structures at Skildingahólsveggur, but dipping to the west (Map 1).

However, south of Stórihver, a second graben, slightly wider than the northern one, seems to exist. The western boundary of this graben is obvious in the older Hamrahlíð fault. We define its eastern boundary as coinciding with the northerly small-scale faults and open fractures to the southwest of Tjarnarás (Map 1). We call this segment of the graben Litlahversmór, which is filled by both the 2600 yrs. Þeistareykjahraun lava and the 11.000/11.400 yrs. Borgarhraun lava. If these two segments are the same graben, then their axes are noticeably shifted. In fact, Gíslason et al. (1984), Sæmundsson (2007) have observed this shift. Sæmundsson (2007) and Sæmundsson et al. (2012a) suggest that the northern segment is shifted 4 to 5 km to the west on a WNW/NW fault. From the description of the author one may understand this shift to be a sinistral motion on the specific fault, even if the fault is parallel to the HF that has a dextral motion.

We see two options for this shift. Either the two grabens are not the same and thus not shifted. Or, if there is a shift, the motion is more complicated than suggested by previous authors. Within the limit of our preliminary analysis we see it likely that these are two different segments. The Skildingahólsveggur fault in the northern segment is dipping to

the west. If its trace is followed southwards, then it runs into the Hamrahlíð or Skeiðin normal faults, which are eastward dipping and are the western boundary of the graben. On the other hand, the eastern flank of the northern graben has five prominent faults striking northerly and northeasterly, all dipping to the west. No obvious equivalent to these faults is to be found in the southern graben, even if the last fault to the east (Klifveggur) matches the eastern boundary fault of the southern graben. A weak zone of roughly 2 km width separates these two grabens, and could be perpendicular to the northerly rift fissure swarm. Whether it is striking WNW or NW cannot be confirmed. The point to remember is that the faults to the north of this ~ 2 km weak zone may not extend southwards under Stórhver. There are a few small-scale normal faults within the southern graben. Their traces are obvious in the Borgarhraun lava farther south, but less obvious in the Þeistareykjahraun to the south approaching the 1.5 km weak zone. Nothing points to the northward extension of these northerly faults under Stórhver. More structural analysis is needed to fully depict the geometry and the mechanism of emplacement of these northerly grabens.

- We observe important features along the NNE and ENE sets at the interval of $N21^{\circ}$ – 70° E, which have not been emphasised previously. The NNE fractures are less common than the ENE fractures (Figs. 7b and 7c) but open fractures strike far more NNE than ENE. As mentioned earlier (Figs. 11a to 11c), in the interval of $N21^{\circ}$ – $N50^{\circ}$ E, the fractures display convincing evidence of sinistral motion based on the geometry of the open fractures. On figure 13, we highlighted where such geometry was observed along this set in the study area. The ENE fractures are as common as the northerly rift-parallel fractures (Fig. 7c), and they are spread almost regularly throughout the study area (Fig. 14). In many places, we observe that the NNE sinistral strike-slips are very near or above the ENE fractures. Therefore, we consider that the interval of sinistral motion is $N21^{\circ}$ – $N70^{\circ}$ E (Fig. 18b), but that the surface expression of this motion is most visible along relatively few fractures at the interval of $N20^{\circ}$ – 40° E. It is possible that the NNE fractures with a strike nearer to $N21^{\circ}$ E blend with the purely extensional northerly fractures of the rift. Similarly, the northerly fractures of the rift whose strike is near $N21^{\circ}$ E may present a component of sinistral strike-slip. Without making a definite statement, most of the NNE fractures seem to dip towards the northwest, and most of the identified dip directions along the ENE set are towards the southeast (Map 1).
- The E-W set, mostly observed at $N81^{\circ}$ – 95° E, is the least common set as seen from statistical analysis (Fig. 7c). The E-W set appears also less frequent at a regional scale (Fig. 15) compared to other sets highlighted on similar maps (Figs. 12 to 14, and 16 to 17). The older E-W faults to the western part of the study area have prominent dip-slips, but in the younger lavas to the centre and east, this set is subtle with hair-line trace and small dip-slip. Almost no open fracture strikes E-W.
- The WNW fractures are as frequent as the rift-parallel fractures (Figs. 7c, 12, and 16). Contrary to common conceptions, the trace of the Húsavík Fault (HF) is straight, striking WNW (Figs. 16 and 18a). The same applies to all other WNW fractures, almost constantly striking at $\sim N121^{\circ}$ – $N130^{\circ}$ E with little deviations. The WNW fractures are regularly spread throughout the area. Dip-slip was identified on many individual segments indicating a dip-direction mostly towards the southwest, i.e., similar to the HF (Fig. 18a and Map 1). In the younger lavas, the WNW fractures have mostly dip-slip, and as mentioned earlier,

few dextral-slip motions could be identified from the geometry of open fractures (Fig. 10a). Concerning the Stórhver, the crater itself is mostly elongated WNW, although a short N100°E fracture exists to the north of it. But the structure is more than just an eruptive crater. On the images, we observe a subtle high in the topography controlled by a longer WNW segment, which summit is the crater. The high appears as a ridge from where a number of lava channels flow to the north and south (Map 1). This means that the last postglacial eruption occurred within the centre of the northerly fissure swarm on a WNW segment perpendicular to the rift (Figs. 12, 16, 18). Our results bring more evidence to the existence of a WNW structure transverse to the northerly fissure swarm as suggested earlier by Sæmundsson (2007). We see the structure being at the latitude of Stórhver. Even in the older crust of north Iceland, WNW transform-parallel fractures, i.e. dykes, are known to be pathways for magma channels (Young et al., 1985).

- NW is a relatively common set, as it can be better seen on the 1° interval diagram on Fig. 7b. The set is regularly distributed in the entire area and has important significance (Fig. 17). NW fractures have among the highest dip-slips in the older series to the west where they control the topography sharply particularly between Mælifell and Hamrahlíð. Additionally, this set presents the highest number of young open fractures in the young and old lavas after the northerly set (Map 1). Three of the most prominent NW striking structures are the open fractures to the east of Höfuðreiðarmúli, the open fractures between Grísatungur and Sæluhúsmúli (Figs. 10a and 10b), and the normal fault in Tjarnarás. But open fractures of this set appear in many places, blending often with the northerly set. As mentioned earlier, the structures of Grísatungur and those to the north in the highland have a left-stepping en échelon arrangement characteristic of a dextral motion (Fig. 10b and 10c). There are two possible motions along the NW fractures. One possibility is that several parallel NW normal faults re-opened locally along the direction of NE due to the dextral motion on the HF. Note that in this case their opening is almost perpendicular to the spreading direction. The other possibility is that the NW fractures at Grísatungur-Sæluhúsmúli have indeed a dextral component that explains their left-stepping en échelon arrangement. The fractures of Grísatungur-Sæluhúsmúli in particular align well with the NW normal faults of Tjarnarás, which on their own have a subtle dextral arrangement. Overall, in the study area, most of the identified NW fractures dip to the west-southwest, although from Hamrahlíð towards Höskuldsvatn a few major faults dip to the northeast (Fig. 18a). If strike-slip occurs indeed along this set as well, then the interval of dextral motion ranges from ~N110°E to N160°E (Fig. 18b).

Finally, a very quick look at the fracture map of Gíslason et al. (1984), also prepared from aerial photographs, shows the same sets of fractures as suggested here being present in the bedrock. Although the authors did not expand their work into the 2600 yrs. old Þeistareykjahraun, which may give a wrong impression that the area was not subject to deformation over this period, at least their map shows the WNW / NW and NNE sets cutting the 11.000 yrs. old Borgarhraun lava.

6 Brief correlation with earthquake and borehole data

Identifying the fracture pattern took longer time than anticipated due to preparation of this large data set in GIS. Therefore, less time was spent on interpreting structurally the pattern itself as well as correlating with additional data. Below, we correlate our results briefly with earthquakes and with selected borehole data. We stress that a thorough correlation with other fracture maps, geophysical and borehole data is necessary using the same structural approach as in this study.

6.1 Earthquake data

Two types of earthquake data are discussed here, the relocated earthquakes within Þeistareykir field (Fig. 19), and the regional data (Fig. 2).

Relocated earthquakes of $-0.6 \leq M \leq 3.2$ in Þeistareykir (Hjaltadóttir and Vogfjörð, 2011) are reported on our raw fracture map (Fig. 19a), and then as four clusters as suggested by the above authors (Fig. 19b). Cluster one stretches from northeast of Tjarnarás to Skildingahóll. Cluster two is between east of Stórhver and northwest of Bæjarfjall. Cluster 3, mostly on the western slope of Bæjarfjall, is complex but seems imprinted on the slope. Cluster four is spread on the northern slope of Bæjarfjall. The traces of the source faults suggested by Hjaltadóttir and Vogfjörð (2011) are highlighted on figure 19b, and the possible motions and the depth of the earthquakes on figures 19c and 19d. These earthquakes occur at a depth of 3 to 7 km for which Hjaltadóttir and Vogfjörð offer complex and sometimes non-conclusive motions. Their description is reported below, followed by our interpretations highlighted *in Italics*.

- The focal mechanisms proposed for cluster one (Hjaltadóttir and Vogfjörð, 2011), are reverse-sinistral, normal-dextral, or reverse on two NW fault segments that have a clear left-stepping en échelon indicative of dextral motion (Figs. 19c and 19d). *These two NW segments coincide with our mapping of a fractured zone with a NW strike (Figs. 19a and 19e). Based on our interpretation of the fracture pattern, we favour the dextral-normal interpretation along these NW segments.*
- Cluster two is nearly spherical in shape for which a WNW source fault is proposed without any specified motion. *At the time of these earthquakes between 2008 and 2010 an uplift occurred near this area, which source was estimated to be at 8.5 km and at 65.88734°N and 17.00733°W (Metzger et al., 2011). These coordinates correspond to $65^\circ53'14''\text{N}$ and $17^\circ0'26''\text{W}$ on Fig. 19a, and are at roughly one kilometre to the north-northwest of the cluster two of earthquakes. The cluster two of earthquakes appears to the southeast of Stórhver crater, and we interpret it as being on the trace of our suggested WNW dextral segment (the Ridge) on which the Stórhver eruption likely occurred (Fig. 19a and e). The WNW segment stretches into the middle of Bæjarfjall (Fig. 19c). A similar idea of possible magma injection on a WNW structures at the latitude of Stórhver has been suggested by Sæmundsson (2007).*
- Cluster three has three segments striking NW, northerly, and WNW. The focal mechanisms offered are reverse-dextral for both the NW and northerly segments. But two options are given for the WNW segment, i.e., reverse-dextral (Fig. 19c), or normal-sinistral (Fig. 19d). *We consider a motion with normal-dextral on the NW segment to the northeast of Tjarnarás more likely since these are the motions that we identified based on the visible en échelon*

segmentation of the NW fractures at Grísatungur-Sæluhúsmúli (Figs. 10b, 10c, and 19e). We see the northerly segment coinciding with our suggested northerly fractures to the west of Bæjarfjall. But we consider that this segment fits better with cluster four, therefore, we discuss its significance below. As to the WNW segment, it is important to recall that the segment is parallel to the HF, which has a known dextral motion. Therefore, we suggest that this segment is rather dextral.

- For the fourth cluster north of Bæjarfjall also two options are suggested (Hjaltadóttir and Vogfjörð, 2011). Either the earthquakes occurred on a long ENE segment with reverse-dextral motion (Fig. 19c), or on two parallel northerly segments one with normal-sinistral and the other with reverse-dextral motions (Fig. 19d). *There are some inconsistencies in these suggestions, however. Firstly, the strike of the northerly segments is that of the rift, but strike-slip motions are suggested for them. Secondly, opposite strike-slip and dip-slip motions are suggested by Hjaltadóttir and Vogfjörð for two parallel and so near fracture segments. These inconsistencies may reflect the uncertainties on the real strike and motion of the source fault. Based on our observations we suggest that if the source faults are shorter northerly segments, then their motion must be rather sinistral and their strike near that of the NNE sinistral fractures. In fact, if the northerly fracture of cluster 3 is taken into account, three “northerly” parallel en échelon segments lay on the trace of the ENE segment to the north of Bæjarfjall, indicating a sinistral motion on the ENE segment (Fig. 19d). If the source fault strikes ENE, then it falls within the strike of our suggested sinistral strike-slip faults (19e).*

Finally, regional earthquake data too show that all the fracture sets that we suggested from aerial imageries are active, and that they rupture during earthquakes with focal mechanisms indicative of strike-slip motions (Figs. 2 and 18b).

The overall conclusion from this comparison is that the great majority of fracture sets present strike-slip motions as determined from the structural analysis and the quick analysis of relocated and regional earthquake data. But further structural analysis is needed to fully understand the tectonics and the earthquakes.

6.2 Well ÞG-8 as an example

Nine deep wells have been drilled at Þeistareykir for exploration and appraisal (Fig. 1a), with a maximum drilled depth of 2659 m (2309 m b.s.l.) for vertical wells and 2456 m true depths for the inclined ones. Within the limit of this report, only one well, well ÞG-8, is chosen for a brief correlation. Well ÞG-8 is the westernmost of the nine wells and is inclined. The well site was chosen with respect to the TEM-MT model of the field. Based on the work of Magnúsdóttir and Brandsdóttir (2011), the drilling targets were potential N-S fractures and eruptive fissure at Stórhver under the Þeistareykir lava field (Mortensen et al., 2011; Blischke and Árnadóttir, 2012). Well ÞG-8 is the coldest of all, with a formation temperature that is inverted below 500m, likely indicating convective cooling (Fig. 20a). Televiewer data were collected at a shallow, then at a deeper level in the well (Blischke and Árnadóttir, 2012). We correlate our results with the well and televiewer data below.

6.2.1 Well data

Well ÞG-8 encountered a succession of glassy basalt, basaltic breccias, basaltic tuffs, and fine to coarse basalts, variably altered, along with eight thin intrusions (Níelsson et al., 2011). Nine aquifers are identified in the well and it seems that only one of them coincides with an intrusion. Therefore, the other aquifers are likely associated with faulting.

- If the main drilling target was a northerly fracture (eruptive or not), then there is a geometrical issue. Assuming that the major northerly fractures on the eastern flank of the northern graben, or those bounding the southern graben stretch beneath the 2600 yrs. Peistareykjakraun lava, the traces of these specific northerly structures do not cross Stórhver but fall either farther west or east of this crater. Secondly, there is a doubt that the eruptive fissure is northerly. As suggested earlier (Figs. 12 and 18), the eruption of Stórhver occurred likely on a WNW dextral strike-slip segment within the centre of the southern graben (Fig. 19e). If our suggestion is correct, well ÞG-8 did not reach the WNW eruptive fissure but ran parallel to this segment and adjacent to a short N100°E fracture (Figs. 20a and 20b).
- It is unlikely that well ÞG-8 crossed the suggested WNW eruptive fissure of Stórhver. Therefore, we checked if our other mapped fractures on the path of this well can be correlated with the aquifers in the entire well. On Fig. 20a, we highlighted and numbered 12 fracture segments that intersect likely well ÞG-8. The E-W segment north of the well that could be a splay fracture of the main WNW eruptive fissure is also numbered (13). This segment runs parallel and is adjacent to the well. It could intersect the well path in a long section between 758 m and 1848 m drilled depth (Fig. 20c). Most of these highlighted fractures are parallel and form weak or fractured “zones” striking ENE, NNE, NW, and northerly (Fig. 20b). All relevant segments and zones are coloured according to their strikes using the same codes as on maps in Figs. 12 to 17. The same colours are also used in the table of Fig. 20c for coherency. The number of fracture segments within each “zone” varies between 1 (the westernmost ENE and northerly) and a maximum of 6 (the zone in the middle of Fig. 20b).
- To check: (a) whether the traces of our suggested tectonic fractures and zones can be found in the well, (b) if these structures correlate with the feeders reported in the well, we used a simplified method in which we read at what distance from the well head (dfwh) our fractures intersect the well path at the surface. Then we calculate their equivalent in terms of drilled depth in order to compare with the depth of the feeders (table of Fig. 20c). The dip direction of most of the suggested fractures is unidentified. However, the ENE segments 6, 6–8, and 11 dip towards the SE, indicating that the entire zone could have a dip to the SE, i.e., towards the well path. As two of the NW segments dip to the West-Southwest, it is likely that the other two NW segments nearest to the well also have the same dip direction (Figs. 20a and 20b).
- In our extensive field mapping in the eroded parts of West and South Iceland we observed that faults and fractures are steeply dipping, generally 75° to 90°, but mostly 80°/85° to 90°. Identical dip values are also reported from televiewer data in well ÞG-8. Therefore, it is reasonable to assume that our suggested fractures also dip steeper than 80°, likely 85° on average. It is reminded that an individual fracture is not a single thin plane, but generally a broken zone of a few centimetres to metres. Nor is an individual fracture stretching straight down into the crust, but has a variety of geometry including segmentations. Considering that the fractured zones here consist of several parallel segments, the width of the broken zones can reach several tens of metres.

- The depth at which a fracture intersects a well depends on the dip value of the fracture. For a fracture dipping towards the wellhead the point of intersection is shifted 190 m to 150 m (drilled depth) for every 5° deviation from the vertical. Fig. 20c shows how our suggested fractured zones and the 13 segments correlate in the well. Three depth-intervals are particularly relevant if we assume that fractures dip 85° to 90° and that they are not single planes but much wider broken zones: (a) The main feeders at the drilled depths of 1680 m to 1688 m and those at 1741 m and 1773 m (603 m to 655 “dfwh”) match our suggested ENE fractured zones containing segments 6 to 8. (b) The minor feeder at 1970 m drilled depth (730 m “dfwh”) matches our segment 9 striking N150°E. (c) Another minor feeder at 2430 m (950 m “dfwh”) would coincide with our suggested fracture N08°E (Fig. 20c). The northerly segment is discussed further in the section below.

Although these considerations are hampered by the uncertainty of the real dip values and the width of the fractured zones, the correlation with feeders tends to support that the suggested fractures have a high chance to be of tectonic origin. In particular, the ENE fractured zone, likely dipping to the SE, gives possibly the permeability at depth as it correlates with the main feeders.

6.2.2 Televiewer data

Based on the interpretation of the televiewer images, about 156 fractures (open, tight and broken zones) are suggested in a limited 285 m section between 1498 m 1773 m in the well (Blischke and Árnadóttir, 2012). Given that most of these fractures have little or no aperture, they are likely to be secondary fractures in the fault zones of more major structures. Blischke and Árnadóttir (2012) divide the suggested fractures into two groups: Above 1700 m they strike N02°E to N35°E, and below 1700 m N30°E to N78°E. Fractures in both groups have a dip value between 70°–90° but mostly 80°–90°, which fits our outcrop observations of fractures in general in Iceland. The authors explain the difference in the strikes of these groups in the televiewer data as due to a change in the direction of the stress field.

- In the interval imaged by televiewer, our mapping suggests two major faults striking N65°E and N60°E (segments 6 and 8 on Fig. 20a) within the ENE major “fracture zone”. As stated earlier, this ENE fracture zone coincides with the main aquifers at 603 m – 608 m “dfwh” (Figs. 20a and 20c). However, the major ENE fracture zone is near the 1700 m “limit” set up by televiewer data where the dominant strikes are northerly to NNE. But as the faults are so near that limit, they could as well belong to the lower group. To find out why the ENE set does not appear strongly above 1700 m, we took the liberty of making a few rose diagrams using the azimuths in the Appendix A of the televiewer report (Blischke and Árnadóttir, 2012). We understand that the given azimuths in the appendix are those of the polar axis. Therefore, we subtracted 90° from those values to obtain the strikes of the fractures compared to the north in order to obtain rose diagrams that are comparable with the results of our study. Figures 21a to 21c show respectively the strikes of all the 156 fractures combined, those above, and those below 1700 m. Clearly, the dominant strikes are mainly northerly (N0°–N10°) but also NNE-NE (N21°E–40°E) above 1700 m, and NNE-ENE (N20°E–N70°E) with a peak at N60°E–N70°E below the limit. However, several sets appear which are not emphasised in the report of Blischke and

Árnadóttir (2012). These are NNW (N170°E–180°E), well visible both above and below 1700m, then E-W (N80°E–90°E) and WNW (N100°E–N110°E) that are few but prominent only below 1700 m.

- Given their depths, the fractures suggested by televiewer are in series older than 11.000 yrs., i.e., late Quaternary. If fracture strikes are indeed as interpreted from televiewer images, then three points arise: (a) Interpreted roughly, the fractures above 1700 m seem to be dominated by rifting, and those below 1700 m are identical to our suggested sets of strike slip (except for the E-W) acting as Riedel shears of the transform zone. (b) What could explain the sharp change in the fracture pattern considering that rift and transform mechanism act simultaneously in time? Neither a change in lithology indicates an unconformity around 1700 m separating two series with different tectonic histories and fracture patterns. Nor the roughly 2° change in the stress field indicated in Appendix D of the televiewer report is significant enough to explain such an abrupt change in strikes. (c) Averaging the strikes of fractures with wide intervals in each group is troublesome because the strike-intervals cover sets of fractures that are of different types. As example, the northerly fractures are of rift nature and thus purely extensional, while the NNE to ENE fractures are sinistral and WNW to NNW dextral strike-slips (Figs. 18 and 19e). Therefore, prior to interpreting televiewer logs, it is essential to have an overview of the existing strikes and motions of fractures.
- The televiewer report also presents data on the apertures of the fractures between 1488 m and 1773 m in the well (Blischke and Árnadóttir, 2012) where nine of the broken zones have an aperture between 100 mm to 620 mm. We took the liberty of analysing the broken zones with apertures > 100 mm. On figure 21d, we reported the strikes and apertures of the nine zones, along with the aquifers at those intervals. We also included the two deepest aquifers (at 1751 m and 1773 m) where total circulation losses occur, although the apertures there are < 100 mm. For visual aid, we made two separate rose diagrams of the strikes of the broken zones with apertures > 100 mm above and below 1700 m (Figs. 21e and 21f). Two observations can be made: (a) Although the larger fracture populations show a sharp change in strike above and below 1700 m, the widest broken zones seem to be dominated by northerly and NNE regardless of depth. (b) The total losses in the deeper parts of the well do not coincide with the largest apertures.
- As mentioned in chapter 6.2.1, we identified two minor northerly fractured zones including segments 10 and 12 (Fig. 20a). These segments, however, would intersect the well at a drilled depth of 2038 m and 2407 m, respectively, which is far below the interval imaged by the televiewer. Because these segments are very short at the surface, it is difficult to ascertain if they are surface expression of a much deeper northerly fault. Projecting the traces of these segments northwards coincides clearly with lava tubes to the north of Stórhver. Lava tubes are not considered to be of tectonic origin, and thus they are unlikely to represent a deep northerly eruptive fissure as it was initially speculated under Stórhver.

Even though the structural analysis of both surface and subsurface is still provisional, the overall messages from the above correlations are that: (a) There is a high number of secondary fractures in the well that reflect both rifting and transform faulting, as we suggested from the surface. (b) These fracture sets likely control the geothermal activity. (c)

Prior to costly operations such as drilling or usage of televiewer, the fracture pattern must be well determined. (d) The well data supports that the “lineaments” we observed on aerial images are significant tectonic structures controlling the permeability at depth.

A more thorough correlation with televiewer and with all boreholes is needed to obtain a comprehensive understanding of tectonic that is so critical for the yield of wells.

7 Summary

We identified 10729 fracture segments in series from late Quaternary to present that includes Miocene locally (Maps 1 and 2), based on observations of eight versions of spots images, orthomaps, and aerial photographs combined (Figs. 4 and 5). The work benefited from our extensive field mapping as well as similar fracture analysis from aerial imageries in other areas of Iceland (e.g., Khodayar et al., 2004; Khodayar et al., 2011). The total number of fractures cutting the rocks is, however, less as a single fracture consists of several shorter segments along trace (Fig. 8). While major segments are prominent in the landscape, the more discreet fractures can either go undetected or be mistaken for cooling fractures, which explains why a part of these fractures cannot be mapped in the field. In order to avoid misunderstanding, we present here a tectonic lineament map rather than a geological map, which is made from outcrops.

The tectonic pattern we obtained is similar to that of Gíslason et al. (1984), which had only the advantage of aerial photographs. Both works show that several fracture sets are present in the study area in addition to the northerly rift-parallel structures. Our work also agrees with the Peistareykir fissure swarm as defined by Sæmundsson (2007). The preliminary structural analysis of our suggested fracture population reveals new results, some of which are not discussed or emphasised enough previously. A few of these results are:

- The identified fractures are faults, open fractures, or prominent joints as rocks are generally not eroded enough here to expose the dykes. The structural analysis of this pattern shows that six fracture sets exist with variable frequency (Figs. 12 to 18). The northerly fractures are the most common followed by WNW and ENE fractures. The NW and NNE sets are less common and the E-W fractures are the least frequent and the shortest of all (Fig. 7c). The northerly rift-parallel fractures ($N0^{\circ}$ - $20^{\circ}E$) constitute roughly 1/3 of the total fracture population. The other 2/3 is of non-rift character, similar to other areas of Iceland where rift and transform zones act together (Khodayar et al., 2004; Khodayar et al., 2011; Khodayar, 2013).
- Except for a few proposed E-W fractures, all sets of fractures are regularly distributed in the area, appearing as parallel weak zones of major or minor lineaments (Figs. 12 to 17). The sets control the landscape, the lava tubes, the lava channels and the eruptive craters. The HF and its parallel fractures have straight traces and are separate from the NW fractures, which form distinct parallel fractured zones in the area (Figs. 16, 17 and 18).
- All sets have dip-slips and the highest slips are along the northerly then the NW fractures. Open fractures strike mostly northerly, NNE and NW, but less WNW and ENE. Almost no open fractures were observed striking E-W. Strike-slip motions are difficult to identify due to rareness of marker horizons, but we have identified some of these motions on the basis of en échelon geometries of fractures, indicating sinistral or dextral motions. To our

knowledge, these motions have not been previously reported in the study area. We identified sinistral motion along a few NNE fractures. In these cases, the NNE fractures are often associated with ENE weak zones. Therefore, the interval of sinistral faults could be N21°E to 70°E (Fig.18). We observe dextral motion along the WNW set (i.e., parallel to HF), best seen in Sæluhúsveggur, then on the NW set as demonstrated by Grísatungur – Tjarnarás swarm.

- Preliminary correlations with regional focal mechanisms (Rögnvaldsson et al., 1998) and relocated earthquakes (Hjaltadóttir and Vogfjörð, 2011) show strike-slip motions along the same fracture sets as we suggest (Figs. 2, and 19a to 19e). In particular, four strike-slips striking NNE, ENE, WNW and NW are identified both by us and by relocated earthquakes at Þeistareykir.
- All previous maps of this area show that faults, especially northerly, have great sinuosity along their traces. We demonstrated that the pronounced sinuosity cannot be interpreted as a single fracture but results from intersection of several fracture sets with various motions. In fact, under a given stress field, fractures with so varied strikes cannot all be pure normal faults of rift, but some will have specific strike-slip motions (Fig. 18b) depending on their angles with respect to the maximum and minimum stresses.
- The northerly set occupies the width of Þeistareykir fissure swarm. The western boundary coincides with the structures to the north of Skessuskálf, and the eastern boundary with Ketilfjall – Kvíhólafjöll structures. There are two young graben segments within the fissure swarm filled by post-glacial lavas. A shift of the fissure swarm at the latitude of Stórhver has been previously mentioned by Gíslason et al. (1984), and estimated at 4–5 km on a WNW/NW fault by Sæmundsson (2007). If this shift is true, it requires sinistral motion on WNW/NW structures that are known to be dextral and parallel to HF. An alternative could be two different graben segments on each side of a 1.5 km wide WNW weak zone at the latitude of Stórhver (Map 1). This zone in the centre of the northerly Þeistareykir fissure swarm contains a WNW ridge. Likely, the last postglacial eruption occurred on this WNW dextral segment at Stórhver at the summit of the ridge (Fig. 19e).
- Well ÞG-8 intended to cross northerly fractures and eruptive fissure at Stórhver. However, there is no indication on aerial images that the major northerly faults on the eastern flank of the northern graben cross the ~ 2 km wide WNW zone and reach the Stórhver crater (Fig. 12a). Nor do the images show a major northerly fault of the southern graben reaching Stórhver (Map 1). Even if televiewer data show a large number of secondary fractures of both rift and transform characters (Blischke and Árnadóttir, 2012), we suggest that the major fractures intersecting the well are mostly of transform character as their strikes fall within the sets that we identified as having strike-slip motions (Fig. 18). As discussed before, a preliminary correlation with borehole data shows that at three depths in the well the aquifers match our suggested fracture sets (Fig. 20c).

It is critical to conduct a thorough analysis of the fracture pattern itself, then correlate with all boreholes and more detailed earthquake data. So far our preliminary correlations demonstrate that a significant part of our suggested lineament segments are tectonic fractures that are well organised along specific strikes and motions, reflecting the influence of rift and transform faulting on geothermal activity.

8 Recommendations

Peistareykir geothermal field at the intersection of NRZ and TFZ undergoes deformation associated with rifting and transform faulting (Fig. 2), leading to a highly fractured-reservoir. The first step in evaluating better the potential drilling targets is to detect the overall tectonic control of Peistareykir field in its complex geological context. Identifying the fracture pattern and their motions is a good practice before investing in drilling and televiewer logging. The fracture population of Peistareykir and surroundings has not been thoroughly reviewed since the work of Gíslason et al. (1984), and conventional structural analysis has not been carried until now.

The present report offers an overview of the fracture pattern, methodologies to extract them, as well as preliminary correlations with earthquake and borehole data to support the results. Our suggested fracture pattern alone is not sufficient to fully understand the reservoir, least to locate wells. The pattern must be revised after correlation with other available data. As a step forward, we suggest an “affordable” work package for a Phase 2, which consists of:

- Correlating the fracture pattern with the alterations in the northeast part of the area.
- Correlating this fracture pattern with previous similar works, further specific earthquake and borehole data, and more thoroughly with televiewer.
- More specific statistical analysis of the fracture pattern, as well as the structural interpretation of the pattern with the published 3D resistivity.
- Synthesis of the all the results and suggestions for further borehole location.

We are confident that if the work plan for Phase 2 is followed without a gap in time, it brings a more comprehensive understanding of the Peistareykir geothermal field since we have already made a quick look at the suggested tasks.

The benefits of Phase 2 are as follows.

1. Comprehensive understanding of Peistareykir geothermal reservoir and immediate surroundings:
 - The role of rift and that of transform zone for the geothermal field,
 - Understanding of tectonic and geothermal activity at reservoir depths,
 - More precise potential areas and specific fracture targets.
2. Stimulate further research in Peistareykir after Phase 2 is published, including testing our results even within Landsvirkjun.
3. Potential for application in other geothermal areas in similar geological context.

Acknowledgments. This work benefited from discussions with Magnús Ólafsson, Kristján Ágústsson, Finnbogi Óskarsson, Kristján Sæmundsson and Ingibjörg Kaldal. Special thanks to the project managers of ÍSOR, Anette K. Mortensen (now at Orkuveita Reykjavíkur) and Magnús Ólafsson, as well as Ásgrímur Guðmundsson and Egill Júlíusson at Landsvirkjun. The report benefited greatly from the thorough review of Ólafur Flóvenz. We wish also to thank Guðrún S. Jónsdóttir, Skúli Víkingsson and Gunnlaugur M. Einarsson at the GIS department of ÍSOR. Kristján Sæmundsson has given separate comments on our work, but for practical reasons we will deal with those comments separately.

9 References

- Björnsson, A., Sæmundsson, K., Einarsson, P., Tryggvason, E., and Grönvold, K. (1977). Current rifting episode in north Iceland. *Nature*, 266, 318–323.
- Blischke, A., and Árnadóttir, S. (2012). *DG-8 Televiewer and Composite Log Data Analysis: ABI-43 Acoustic Borehole Image and Lithology Log Data Processing and Interpretations for Depth Interval 1493.5–1775 m*. Iceland GeoSurvey, report, ÍSOR-2012/020, 43 p + 2 Appendices.
- Brandsdóttir, B. and Einarsson, P. (1979) Seismic activity associated with the September 1977 deflation of the Krafla central volcano in NE-Iceland. *Journal of Volcanology and Geothermal Research*, 6, 197–212.
- DeMets, C., Gordon, R. G., and Argus, D. F., (2010). Geologically current plate motions. *Geophysical Journal International*, 181 (1), 1–80.
- Einarsson, P. (1979). Seismicity and earthquake focal mechanisms along the mid-Atlantic plate boundary between Iceland and the Azores. *Tectonophysics*, 55, 127–153.
- Einarsson, P. (1991). Earthquakes and present-day tectonism in Iceland. *Tectonophysics*, 189, 261–279.
- Einarsson, P., and Björnsson, S. (1979). Earthquakes in Iceland, *Jökull*, 29, 37–43.
- Garcia, S., Arnaud, N. O., Angelier, J., Bergerat, F., and Homberg, C. (2003). Rift jump process in Northern Iceland since 10 Ma from ⁴⁰Ar/³⁹Ar geochronology. *Earth and Planetary Science Letters*, 214, 529–544.
- Geirsson, H., Árnadóttir, Th., Hreinsdóttir, S., Decriem, J., LaFemina, P. C., Jónsson, S., Bennett, R. A., Metzger, S., Holland, A., Sturkell, E., Villemin, T., Völksen, C., Sigmundsson, F., Einarsson, P., Roberts, M. J., and Sveinbjörnsson, H. (2010). Overview of results from continuous GPS observations in Iceland from 1995 to 2010. *Jökull*, 60, 3–22.
- Gíslason, G., Johnsen, G. V., Ármannsson, H., Torfason, H., and Árnason, K. (1984). *Þeistareykir: Yfirborðsrannsóknir á háhitasvæðinu*. National Energy Authority, report, OS-84089/JHD-16, 134 p. and 3 maps.
- Halldórsson, P. (2005). *Jarðskjálftavirkni á Norðurlandi - Earthquake activity in N-Iceland*. Veðurstofa Íslands, IMO report 05021, 34 p.
- Hjaltadóttir, S., and Vogfjörð, K. (2011). *Sprungukortlagning við Þeistareyki og Bjarnaflag með háupplausnarstaðsetningum smáskjálfta*. Landsvirkjun, report, LV-2011-116, 44 p.
- Jakobsdóttir, S. S. (2008). Seismicity in Iceland: 1994–2007. *Jökull*, 58, 75–100.
- Jancin, M., Young, K. D., Voight, B., Aronson, J. L., and Sæmundsson, K. (1985). Stratigraphy and K/Ar ages across the west flank of the Northeast Iceland axial rift zone, in relation to the 7 Ma volcano-tectonic reorganization of Iceland. *Journal of Geophysical Research*, 90, 9961–9985.
- Karlsdóttir, R., Vilhjálmsson, A. M., Árnason, K., and Teklesenbet Beyene, A. (2012). *Þeistareykir Geothermal Area, Northern Iceland: 3D Inversion of MT and TEM Data*. Iceland GeoSurvey, report, ÍSOR-2012/046, 173 p.

- Khodayar, M. (2009). *Geological map of Hallarmúli volcano, West Iceland, scale 1:20.000: Bedrock, tectonics and unstable plate boundaries*. Iceland GeoSurvey, report, ÍSOR-2009/060, 23 p., 1 Map.
- Khodayar, M. (2013). *Fracture analysis from aerial imageries and correlation with triggered earthquakes by injections at Húsmúli, Hengill, South Iceland*. Iceland GeoSurvey, report, ÍSOR-2013/008, 26 p. and 3 maps.
- Khodayar, M., and Björnsson, S. (2013). Fault ruptures and geothermal effects of the second earthquake, 29 May 2008, South Iceland Seismic Zone. *Geothermics*, 50, 44–65 (first published on line Septembre 2013), <http://dx.doi.org/10.1016/j.geothermics.2013.07.002>.
- Khodayar, M., and Einarsson, G. M. (2006). *Tectonic lineament map of South Iceland between Sultartangi and Thingvellir, 1:125.000*. Iceland GeoSurvey, report, ÍSOR-06145, 4 p., 1 Map.
- Khodayar, M., Björnsson, S., and Franzson, H. (2011). *Hvammsvirkjun, Holtavirkjun, Urriðafossvirkjun: Synthesis of 2001–2010 geological data from Hreppar and South Iceland Seismic Zone*. Iceland GeoSurvey, report, ÍSOR-2011/032, LV-2011/073. 80 p., 11 Maps.
- Khodayar, M., Franzson, H., Björnsson, S., Víkingsson, S., and Jónsdóttir, G. S. (2004). *Tectonic lineaments of Borgarfjörður-Hvalfjörður from aerial photographs, West Iceland: Preliminary results*. Iceland GeoSurvey, report, ÍSOR-2004/021, 47 p., 1 Map.
- Kristinsson, S. G., Friðriksson, Þ., Ólafsson, M., Gunnarsdóttir, S. H., and Nielsson, S. (2013). *Háhitavæðin á Þeistareykjum, í Kröflu og Námafjalli: Vöktun á yfirborðsvirkni og grunnvatni*. Iceland GeoSurvey, report, LV-2013-091, 152 p.
- Magnúsdóttir, S., and Brandsdóttir, B. (2011). Tectonics of Þeistareykir fissure swarm. *Jökull*, 61, 65–79.
- Metzger, S., Jónsson, S., and Geirsson, H. (2011). Locking depth and slip-rate of the Húsavík-Flatey fault, North Iceland, derived from continuous GPS data 2006–2010. *Geophysical Journal International*, 187, 564–576.
- Mortensen, A. K. (2012). *Þeistareykir: Tillögur um staðsetningu borholna í jarðhitakerfinu á Þeistareykjum 2012*. Iceland GeoSurvey, report, ÍSOR-2012/043, 36 p.
- Mortensen, A. K., Gautason, B., Ólafsson, M., Karlsdóttir, R., Ármannsson, H., Egilson, Þ., and Axelsson, G. (2011). *Þeistareykir - Forsendur og tillögur að hönnun rannsóknarholna frá borteigum C og N*. Iceland GeoSurvey, short report, ÍSOR-11049.
- Nielsson, S., Egilson, Þ., Gunnarsdóttir, S. H., Stefánsson, H. Ö., Jónasson, H., Tryggvason, H., and Vilhjálmsson, S. (2011). *Þeistareykir – Hola ÞG-8: 3. áfangi: Jarðlög og mælingar. Borun vinnsluhluta með 8½" krónu frá 1495 m í 2503 m dýpi*. Iceland GeoSurvey, report, ÍSOR-2011/80, 67 p.
- Óskarsson, F. (2011). *Háhitaholur á Þeistareykjum: Efnasamsetning vökva og gufu*. Iceland GeoSurvey, report, ÍSOR-2011/068, 28 p.
- Pálmason, G. (1980). A continuum model of crustal generation in Iceland; kinematic aspects. *Journal of Geophysics*, 47, p. 7–18.
- Rögnvaldsson, S. T., Gudmundsson, A., and Slunga, R. (1998). Seismotectonic analysis of the Tjörnes Fracture Zone, an active transform fault in north Iceland. *Journal of Geophysical Research*, 103, p. 30117–30129.

- Stefánsson, R., Guðmundsson, G. B., and Halldórsson, P. (2008). Tjörnes fracture zone. New and old seismic evidences for the link between the North Iceland rift zone and the Mid-Atlantic ridge. *Tectonophysics*, 447, p. 117–126.
- Sæmundsson, K. (1974). Evolution of the axial rifting zone in northern Iceland and the Tjörnes fracture zone. *Bulletin of Geological Society of America*, 85, p. 495–504.
- Sæmundsson, K. (1978). Fissure swarms and central volcanoes of the neovolcanic zones of Iceland. *Geological Journal, Special Issue*, 10, 415–432.
- Sæmundsson, K. (2007). *Jarðfræðin á Þeistareykjum*. Iceland GeoSurvey, short report, ÍSOR-07270, 23 p.
- Sæmundsson, K., Sigurgeirsson, M. Á., and Grönvold, K. (2012a). *Þeistareykir. Jarðfræðirannsóknir 2011*. Iceland GeoSurvey, report, ÍSOR-2012/024, 61 p., with map.
- Sæmundsson, K., Hjartarson, Á., Kaldal, I., Sigurgeirsson, M. Á., Kristinsson, S. G., and Víkingsson, S. (2012b). *Geological Map of Northern Volcanic Zone, Iceland. Northern part. 1:100.000*. Reykjavík, Iceland GeoSurvey and Landsvirkjun.
- Thoroddsen, Th. (1899). *Major Earthquakes in Iceland* (in Icelandic). The Icelandic literary Society, Copenhagen, 269 p.
- Voight, B., and Mamula, N. Jr. (1983). Structures and tectonics of northern Iceland. In J. E. Estes and G.A. (edits) *Thorley Manual of Remote Sensing, 2nd ed., Vol. 2.*, p. 1782–1786, American Society of Photogrammetry, Falls Church, Va.
- Young, K.D., Jancin, M., Voight, B., and Orkan, N. I. (1985). Transform deformation of Tertiary rocks along the Tjörnes Fracture Zone, North Central Iceland. *Journal of Geophysical Research*, 90, p. 9986–10,010.

ANNEX

Annex to the methodology and use of aerial imageries

Identifying fractures or folds, or even the extent of formations on aerial imageries is a well-known and widely used methodology since long. By necessity, the methodology has matured especially outside of Iceland in terrains that are more often than not covered by vegetation, thus offering poor or no exposures to collect geological data in the field. The success rate of the method has been high be it for exploration (mining, hydrocarbon, or geothermal) or simply geological studies to understand the tectonic.

In Iceland, the coverage by vegetation is not an issue, which means that the series, as well as major dykes and faults are easily observed in the field. However, from own experience of both field geological mapping and large-scale observations of aerial images in Iceland, we know that all structures cannot be seen while standing in the field due to outcrop conditions, or the choice of a geologist as what structure to map in the field. A comprehensive geological work begins with the analysis of the imageries to have an overview of the distribution of the formations and fractures, and continues as a support during field mapping. By experience, we also know that a geological map always presents less fractures than obtainable from aerial imageries for the simple reasons that: (a) It takes less time to map from aerial images than crossing the landscape in the field to reach individual structures; (b) Larger faults and dykes are easier to map in the field, overshadowing the finest fractures, which are also a part of tectonic deformation; (c) Strike-slip faults may be interpreted as a joint in the field and disregarded because of difficulties in finding marker horizons or micro-structures to determine these significant structures. Thus aerial imageries give an overall view of all “breaks” in the rocks, be it a simple joint, a minor fault, or a major fault, all of whom are a response to the stress field.

It is also important to bear in mind that not all the faults are in an identical stage of development. Some faults display longer and sharper traces because they have been active for a longer period of time, accumulating slips and contributing to the shaping of topography. The signature of these ones is more obvious in the landscape. But the younger faults had less time to accumulate slips, are shorter, may have more subtle traces or be less obvious in the topography. But still, they reflect the status of deformation, at a younger stage. Excluding the less prominent fractures because their traces are subtle, an untrained eye may not see them, or these may be misinterpreted as non-tectonic structures leads to missing valuable information that may change the overall interpretation. Therefore, structures must be observed at any stages of their developments, from both the aerial images and the field, by trained geologists without preferences for specific types of structures.

In our study area in Þeistareykir, we mapped about 10729 segments, which are a blend of major and minor fractures. Because the picture they reflect is somewhat different from what has been more commonly offered up to now, the question of their validity as tectonic structures may arise. We have made the best efforts to map only what we estimate to be fractures of tectonic origin. In this regard, we transferred our experience from both field mapping and aerial images observations in other areas of Iceland that present the same types of lavas, faults, dykes, and open fractures as in Þeistareykir. This experience covers as much older fractures as the younger ones, and in a few cases we have been able to observe in the field how a fracture starts as a joint but subsides over 3–4 years to become a fault. If our

suggested fractures in Þeistareykir are of non-tectonic origin, one might suggest that they are one of the following:

- *Man-made or animal tracks.* The area is not populated enough to have a dense network of roads and tracks, nor many ditches for agricultural purposes. The topographic base maps used in our study contain all these pathways and our suggested fractures reported onto these maps do not coincide with the man-made or animal tracks. Interestingly enough, during our field mapping of the source faults of earthquakes in the South Iceland Seismic Zone, often we observed that these young structures are borrowed by animals for the simple reason that these weak zones in the landscape are favorable paths and are easier to use than make. Although of different types, the open fractures of Þeistareykir are not different from those in South Iceland and particularly the finer open fractures, as well as joints, can be used by animals in Þeistareykir as well.
- *Water streams and erosional structures.* It is well known in all areas of Iceland, not the least in geothermal systems that leakages occur on fractures, be it a stream, a local pond or a spring, or a permeable zone at depth. As to the erosional forces, they attack easier a landscape with an existing topography that is a result of fault-slip. In Þeistareykir, erosional phenomena are not so common in the younger lavas < 15.000 years, because these lavas are in a relatively flat low-land with little or no prominent regularities in the landscape to be used by erosional forces. A clear relation between erosion and tectonics can be seen on the geological map of Sæmundsson et al. (2012b). To the north of our study area in a limited zone from Þríhyrningsdalur to Bjargadalur, dry erosional channels are obviously aligned northerly in a topography made by N-S faults. The map even shows that some of these channels are blending with the apparent faults.
- *Flow structure and cooling fracture of lavas.* Other surface phenomena such as lava flow structures are more likely than not controlled by underlying topography, which in turn is controlled by tectonics, or directly coinciding with the youngest fine subtle fractures. As to the cooling fractures in the lava, columnar joints are known to the outcrop expressions of the phenomena. These columns are hexagonal and cool perpendicular to the surface of the lava. The size of each hexagon is generally a few tens of centimetres, rarely exceeding a metre. If they are visible at the surface of the lava, their hexagonal pattern is very similar to desiccation cracks in mud on the ground with less opening and roughness around the contours of the hexagon. Due to their sizes, these columnar joints are not well visible at the surface of the lava on spot or orthomaps from the air. Even if they were visible, their very local hexagonal pattern would distinguish them in the fracture population. However, no such a pattern is observed among the suggested fracture segments in this study for the simple reason that the surface of the lava is not eroded enough to show the hexagonal columns. The statistical analysis does not reflect a hexagonal pattern but preferential strikes that reflect definitely the fracturing of rift and transform zones, besides the facts that fractures, particularly in the youngest 2600 yrs lavas often extend into older lavas and bedrock. Such a fracture has hundreds of metres if not kilometres and can hardly be called a cooling fracture of the lava.

The presence of the above structures does not, however, degrade the methodology itself, nor the results of this study. As a matter of fact, the mapped fractures are presented in our maps as definite when we are reasonably sure of their tectonic origin and “possible” when their traces are more subtle or we are less sure about their origin. It is nevertheless striking that most, if not all of the “possible” fractures on the map fall on the traces of definite structures.

If most of the mapped fractures were of non-tectonic origin, then their strikes would be random in rose diagrams, or the rose diagrams would show an equal amplitude distribution in all directions. But as the statistical analysis in chapter 4 showed, a clear tectonic pattern emerges from our study, reflecting the mechanism of both rifting and transform faulting, and fitting with the regional stress. Interesting enough, the correlation of earthquake and televiewer data in chapter 6 shows a definite fit with our suggested tectonic pattern.

FIGURES

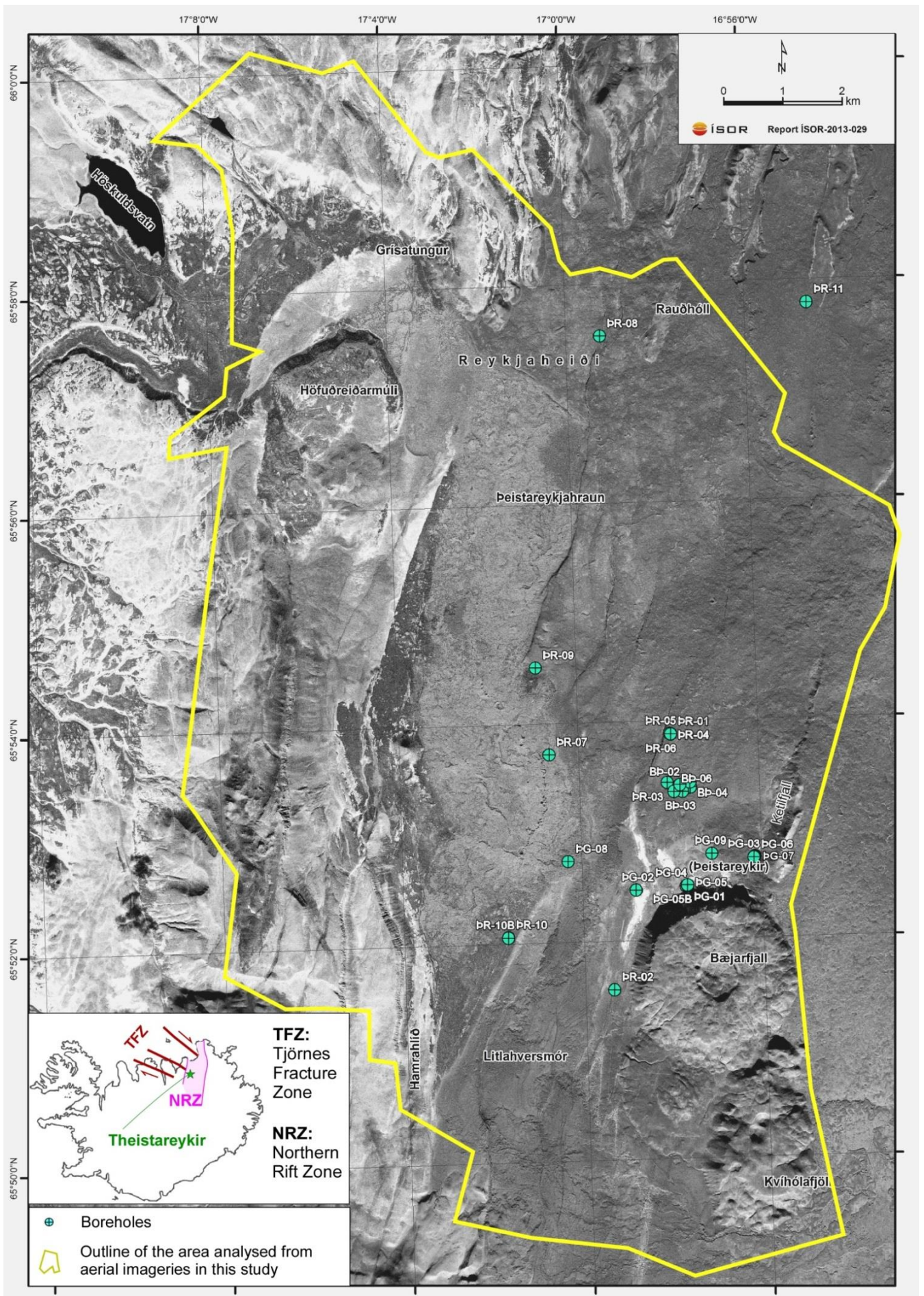


Figure 1. The outline of the area covered by observations of aerial imageries in this study and location of boreholes at and surrounding Þeistareykir.

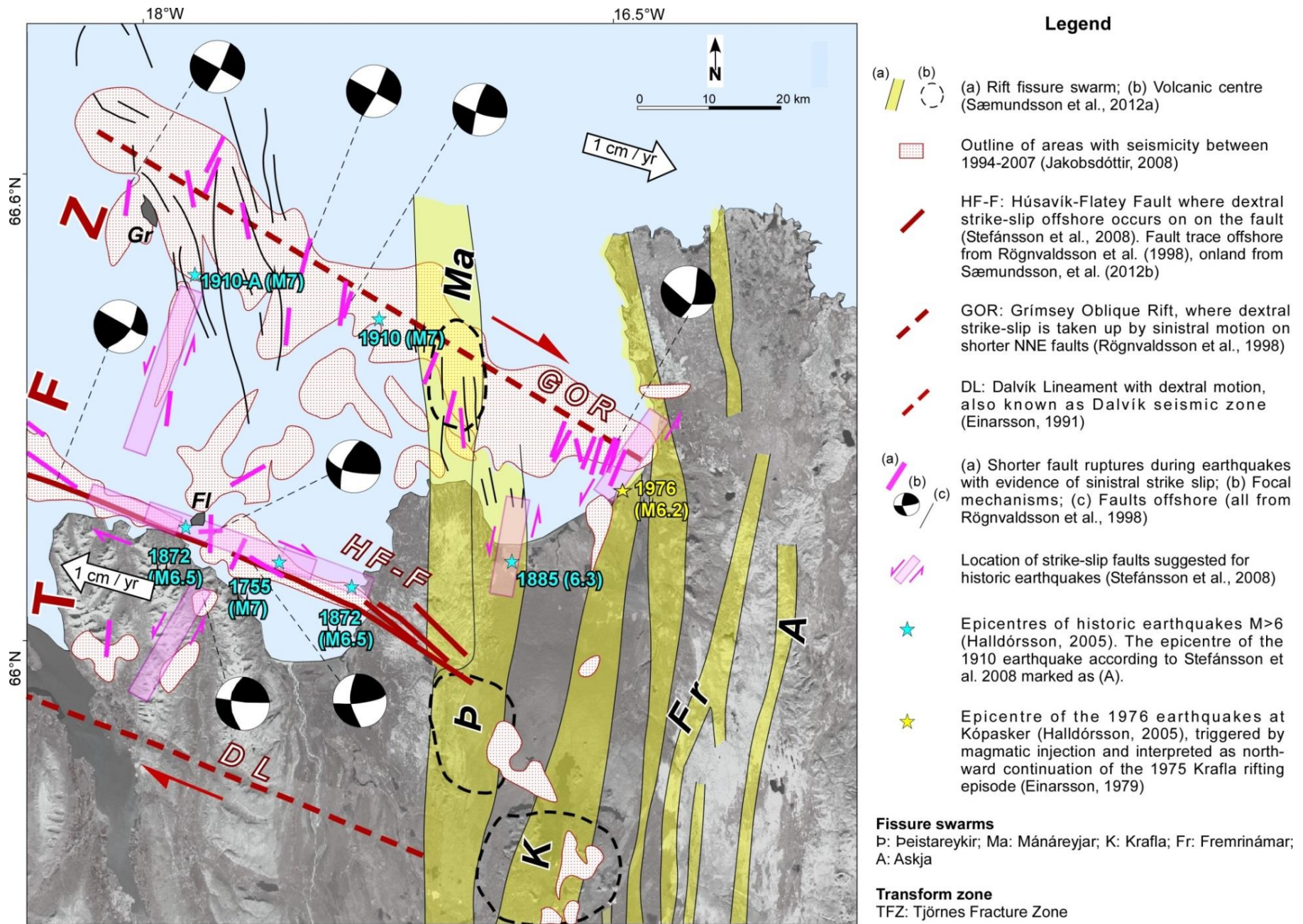


Figure 2. Compilation of tectonic elements of rift and transform zones plate boundaries in North Iceland.

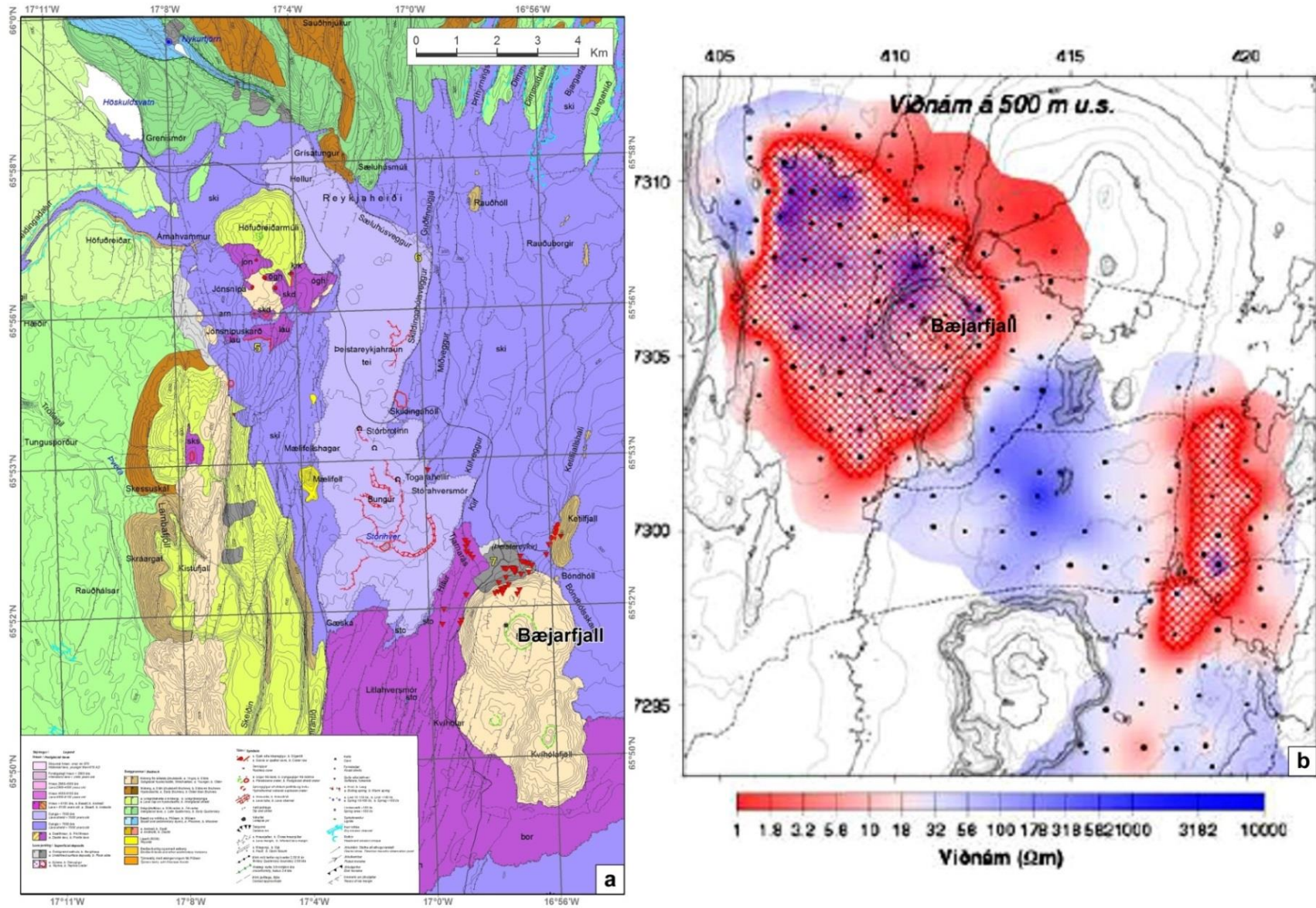
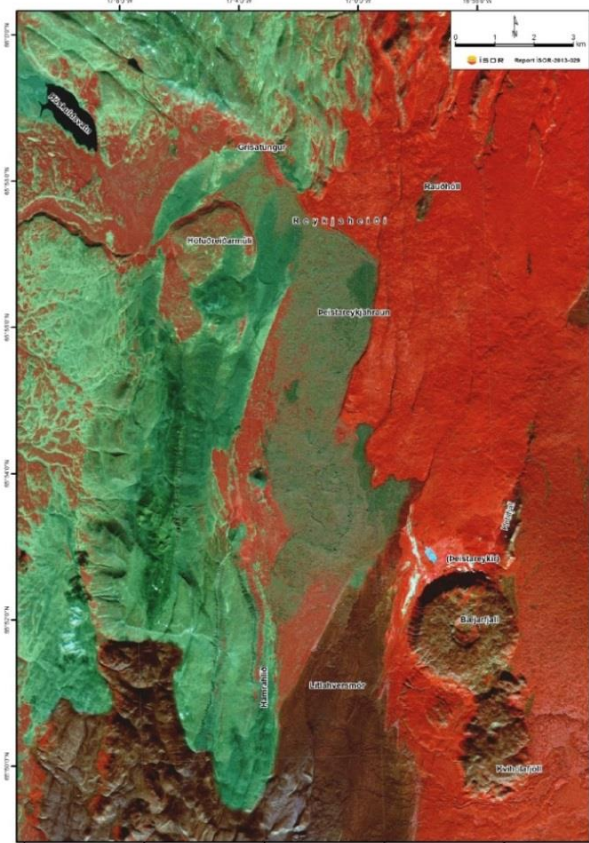
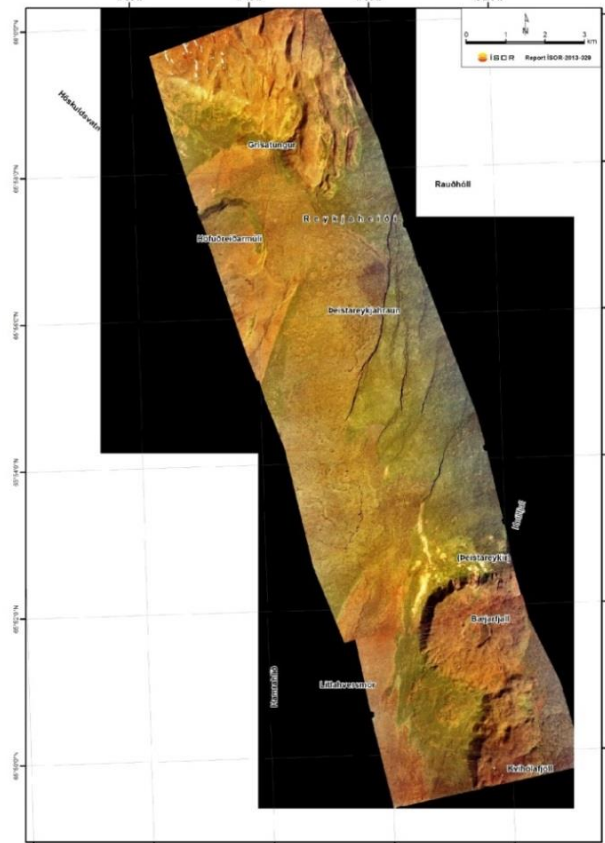


Figure 3. Overview of geological and geophysical studies. (a) Geological map by Sæmundsson et al. (2012b) emphasizing rift parallel fractures. (b) High resistivity core (hatched area) at 500 m b.s.l. under a low resistivity cap, indicative of prospective geothermal field (Karlisdóttir et al., 2012).

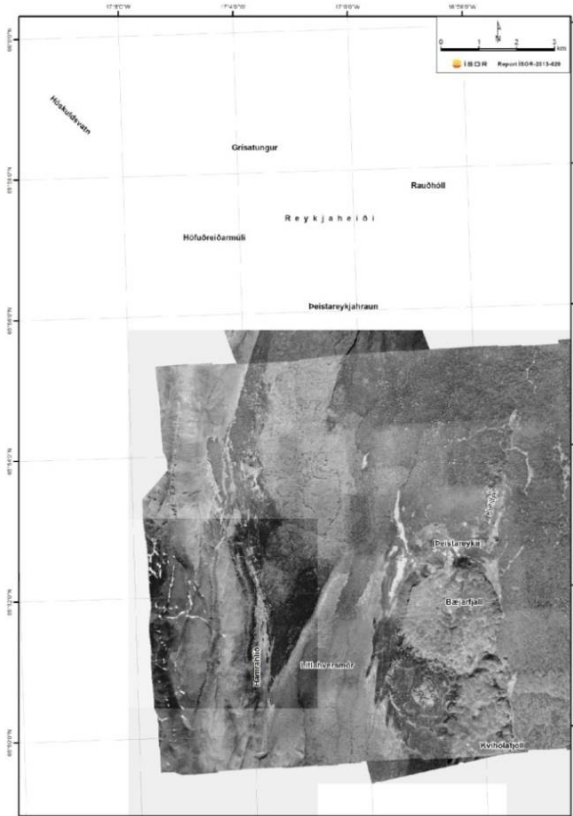
Example of spot (infrared) from 2003



Example of orthomap in color from 1998



Example of orthomosaic in black & white from 2007



Example of aerial photograph (black & white) from 1960 and 1961



Figure 4. Examples of image types used in this study and their coverage on the ground. (a) Spot; (b) Orthomaps from 1998; (c) Orthomaps from 2007; (d) Aerial photographs. See text for explanations.

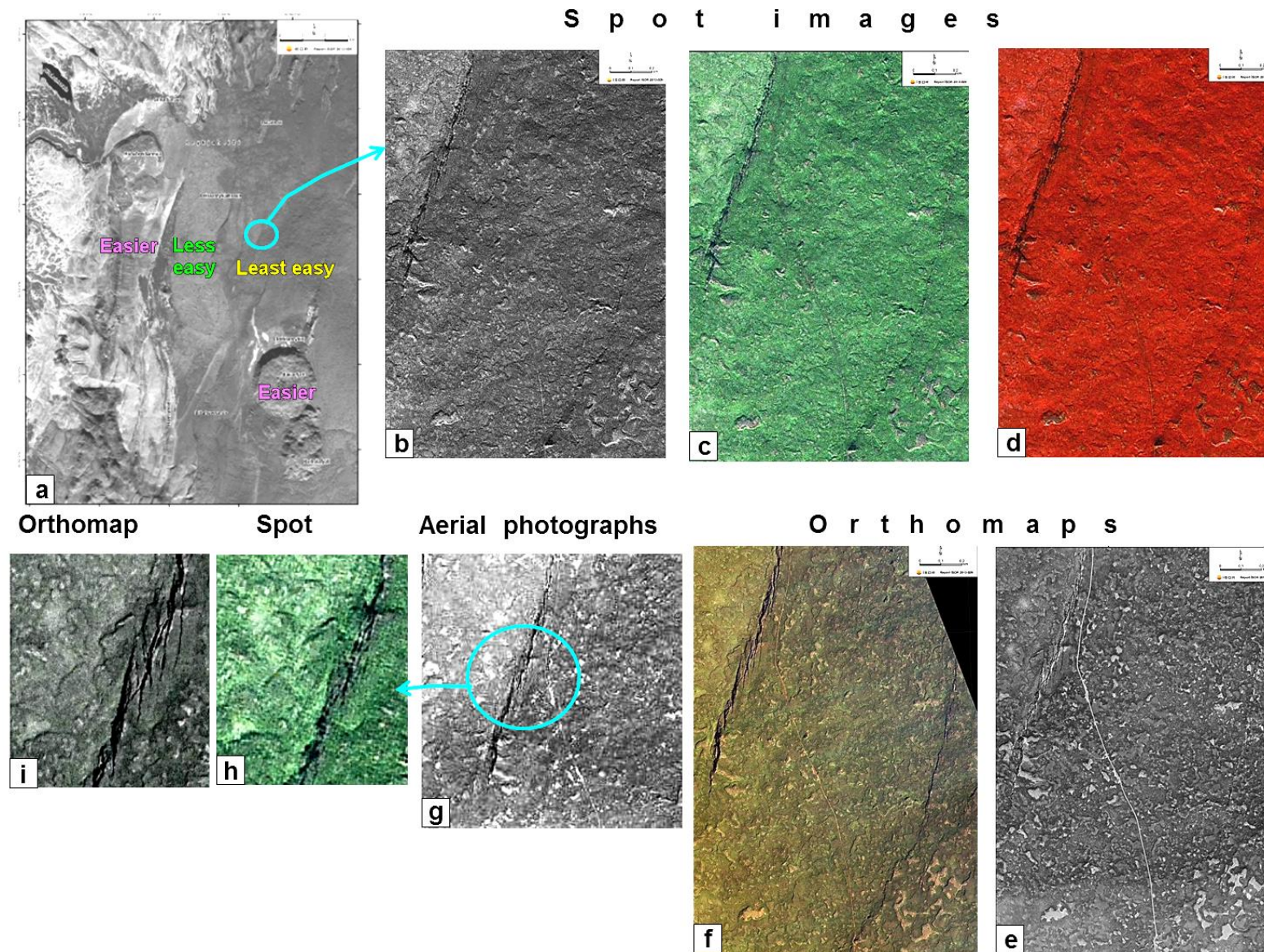


Figure 5. Examples of how structures appear on each image type. (a) The overall easiness of observation in each area. The traces of the structures change slightly or much from: (b) Monochrome, (c) Composite and (d) Infrared spot images to, (e) Black and white, (f) Color orthomaps, and (g) Aerial photographs. Even the strike of the fractures may be slightly different depending on images. Snap shots of: (h) Spot and (i) Orthomap images showing the variation in strike and geometry of obvious and more discreet fractures.

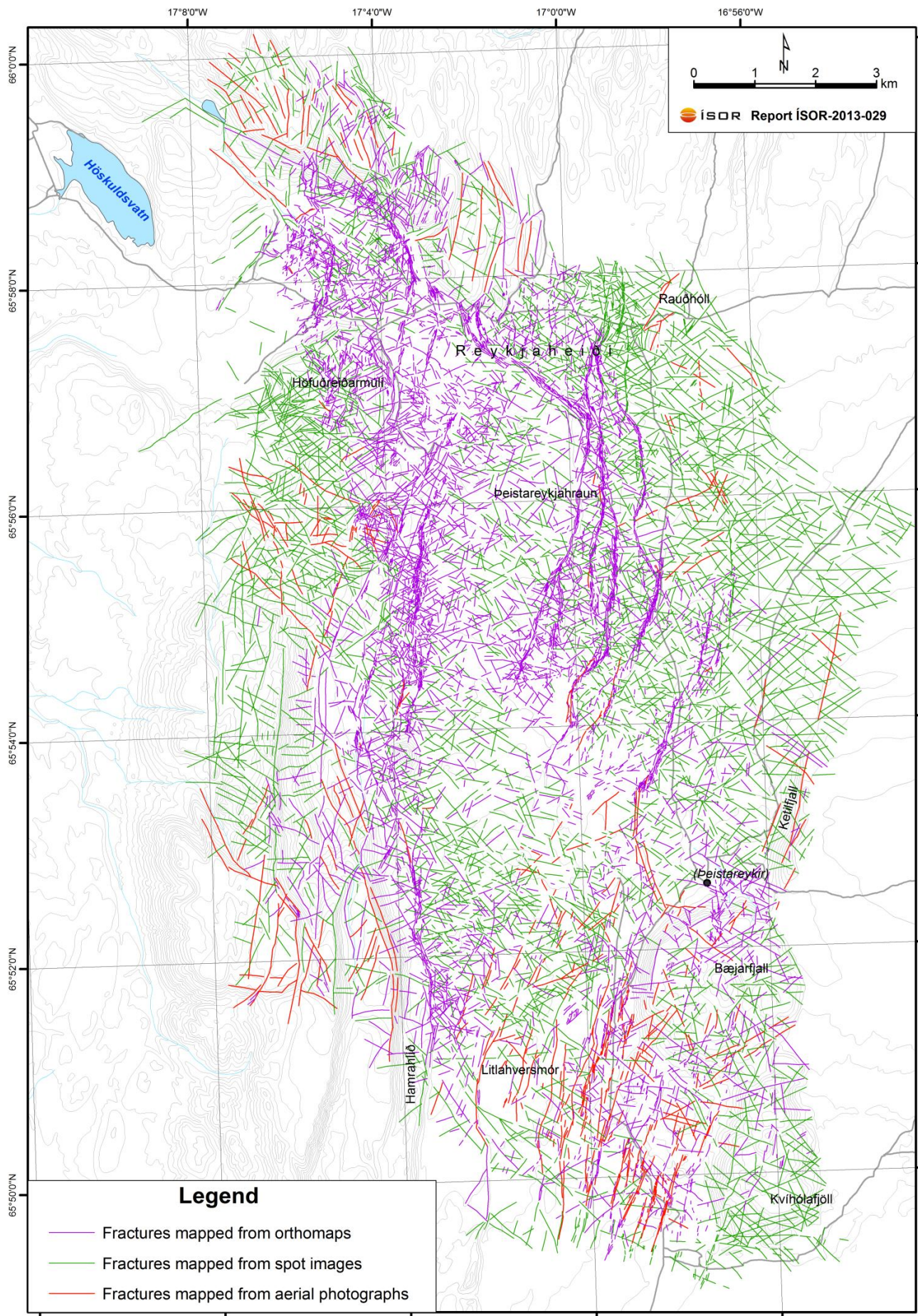


Figure 6. Map showing the type of image used to draw the fracture pattern.

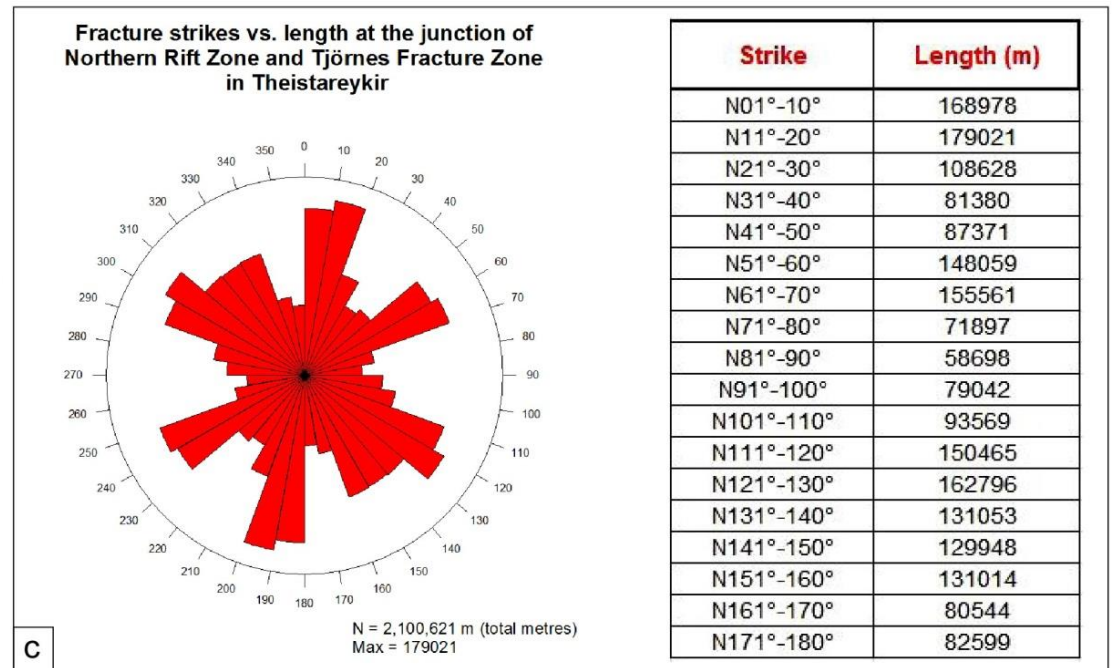
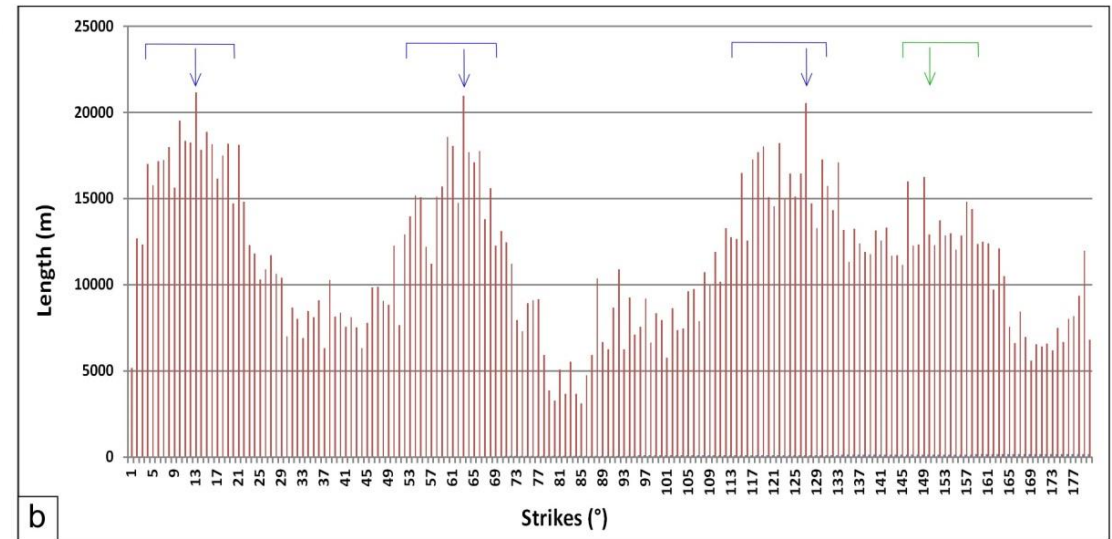
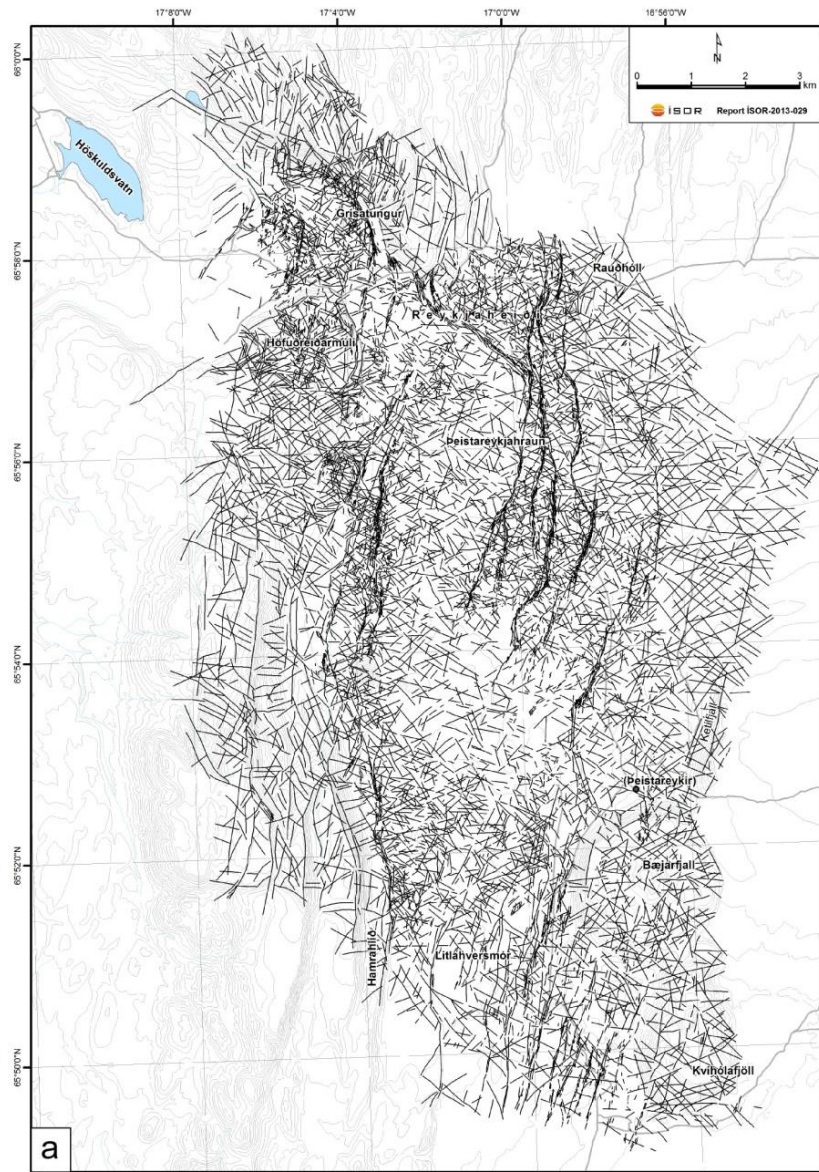


Figure 7. Statistical analysis of the fracture population. (a) Map of the raw fractures. (b) Statistical analysis based on fracture strikes vs. fracture length shown at 1° interval strike. (c) Statistical analysis based on fracture strike vs. fracture length shown on a rose diagram with 10° interval. The data set in the table to the right is also valid for Fig. 7b.

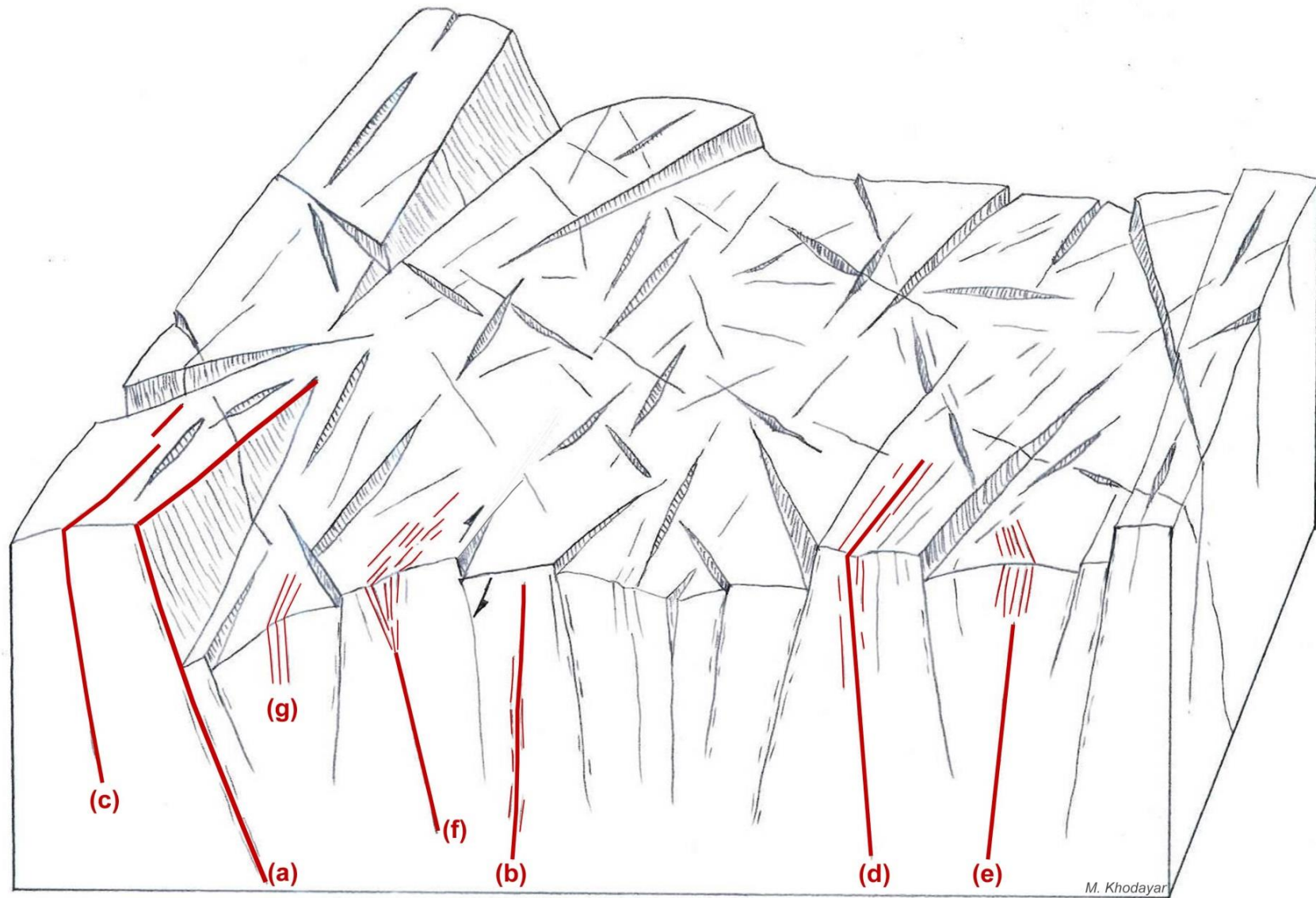


Figure 8. Schematic block diagram made for this study to show possible fracture geometries, their surface expressions, and the resulting horts and grabens. (a) A major fault, segmented, with conspicuous dip-slip and surface expression. (b) A major fracture with rupture at depth but without a surface expression (case of a hidden active fracture). (c) A single segment with major trace. (d) A weak zone with one major plane and several parallel minor planes. (e) Only minor parallel planes dipping in the same direction as the main fracture at depth, (f) Minor planes some with opposite dip directions above a major fracture at depth. (g) Several minor fractures without deep roots.

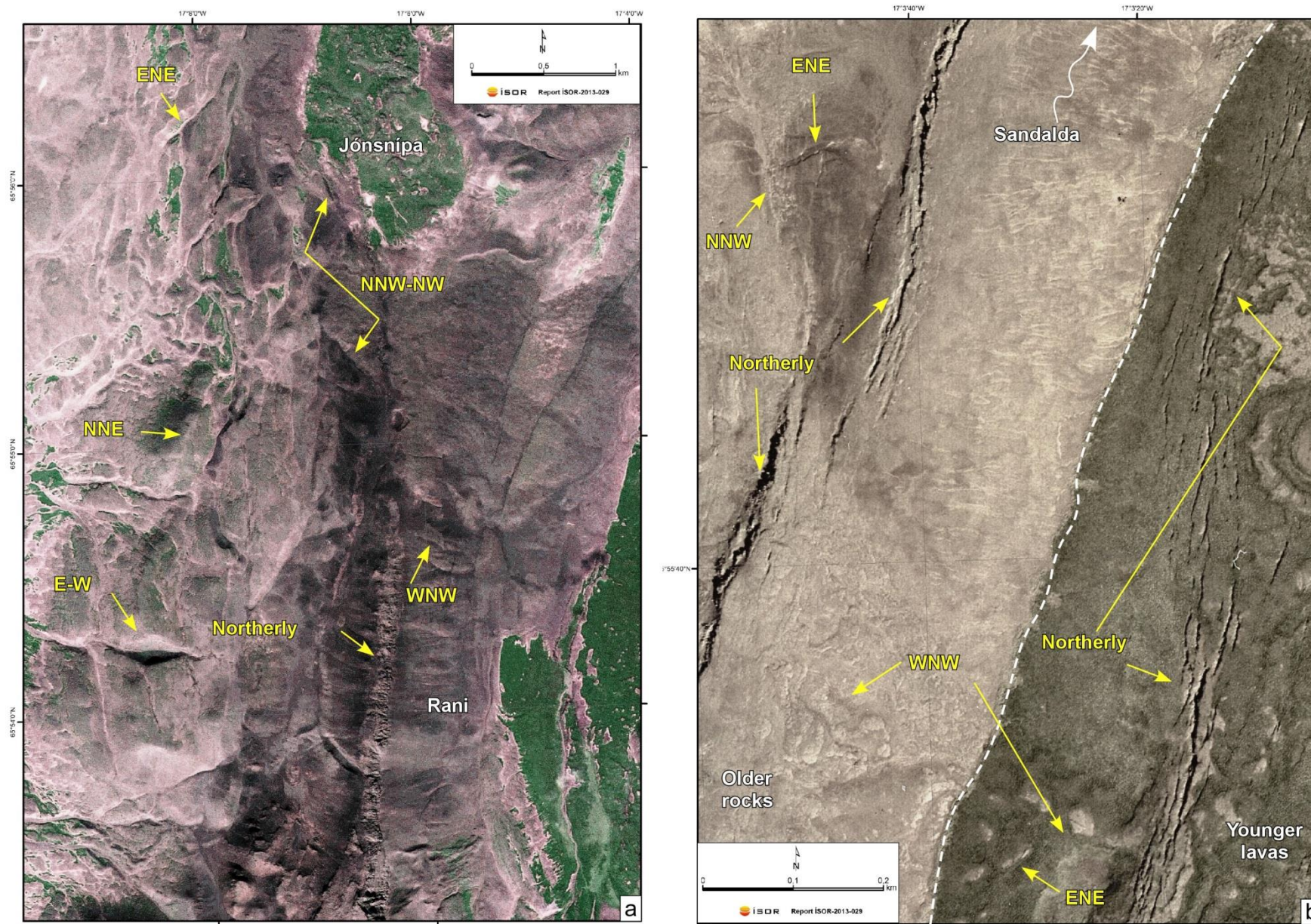


Figure 9. Examples of fractures (1). (a) Examples of ENE, northerly, NW and E-W faults, some with dip-slip, well visible in the older rocks on spot images. (b) Prominent open fractures and young normal faults with small dip-slips in the older and younger lavas (orthomaps). Note other sets of fractures and their subtle surface expressions.

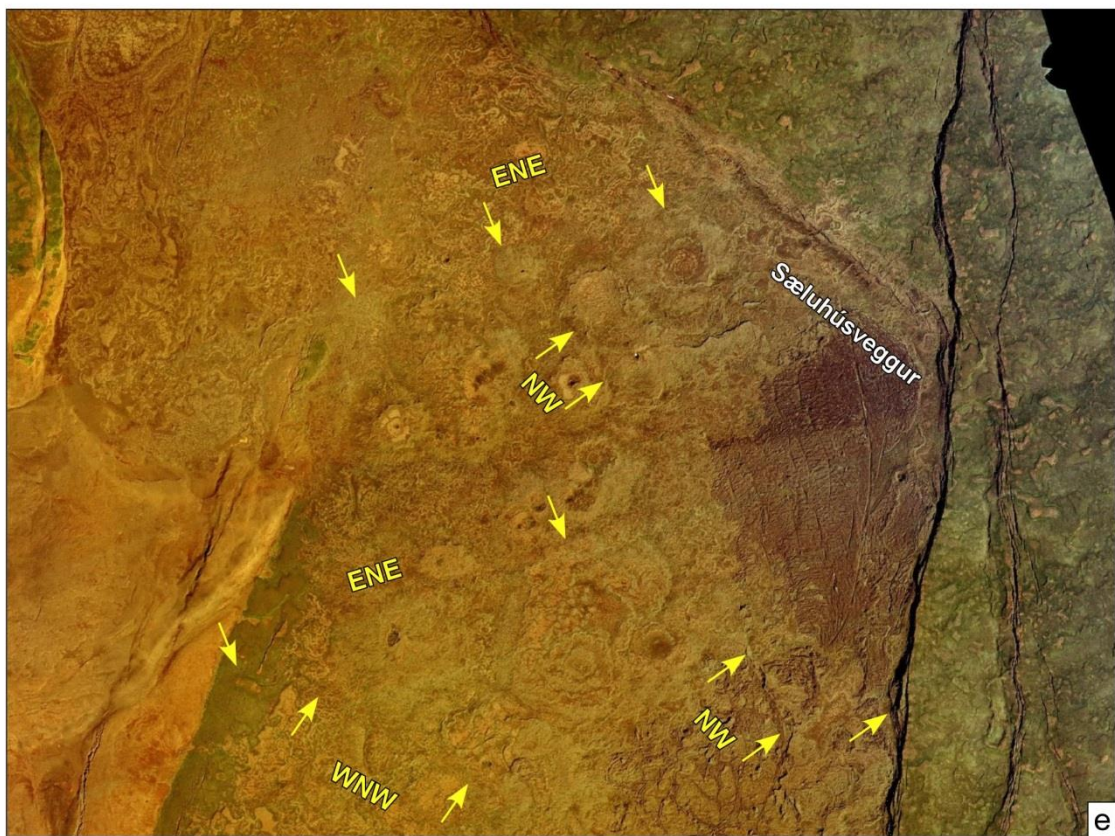
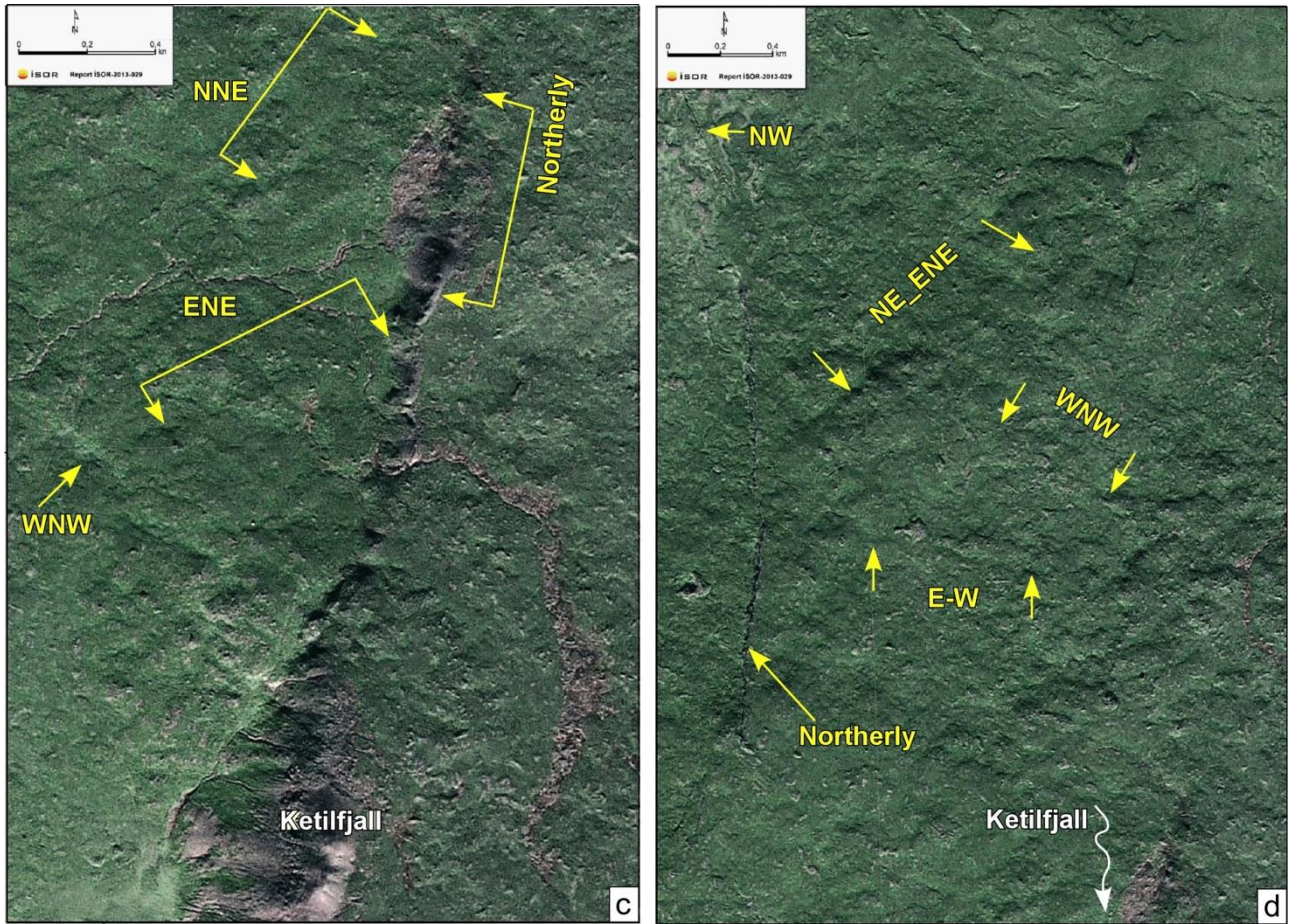


Figure 9. (Cont.). Examples of fractures (2). (c) and (d) Various fracture sets and their surface expressions in the least easy observation areas (spot). The fractures highlighted here are the most obvious in the least easy area. (e) Highlights of young non-rift-parallel fractures with subtle traces in the 2600 yrs. Þeistareykir lava in the “northern graben”. Note their extension beyond this youngest lava.

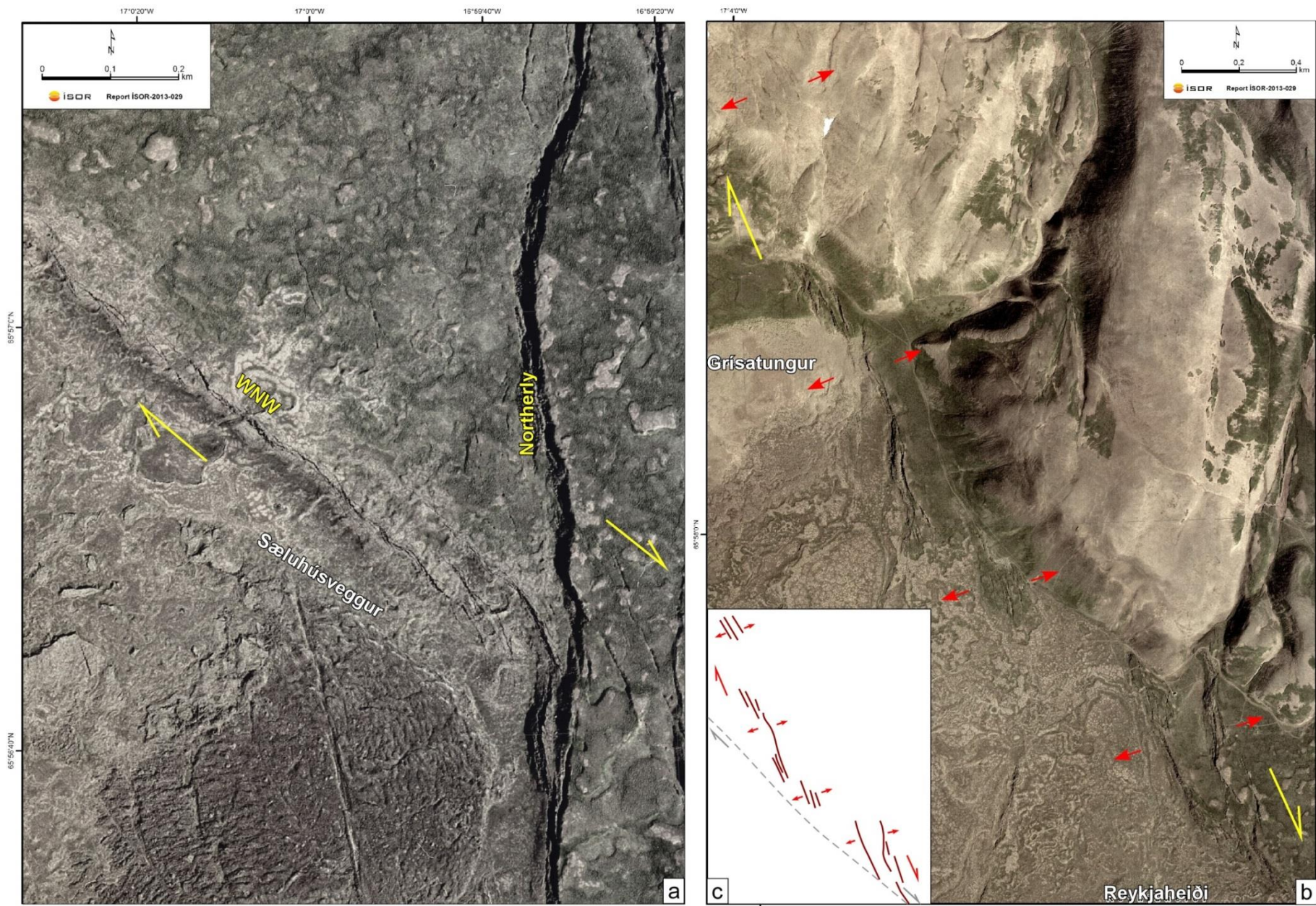


Figure 10. Examples of dextral strike-slips based on the left-stepping en échelon arrangement of open fractures. (a) Along the WNW set. (b) Possibly along the NW set (images are orthomaps).

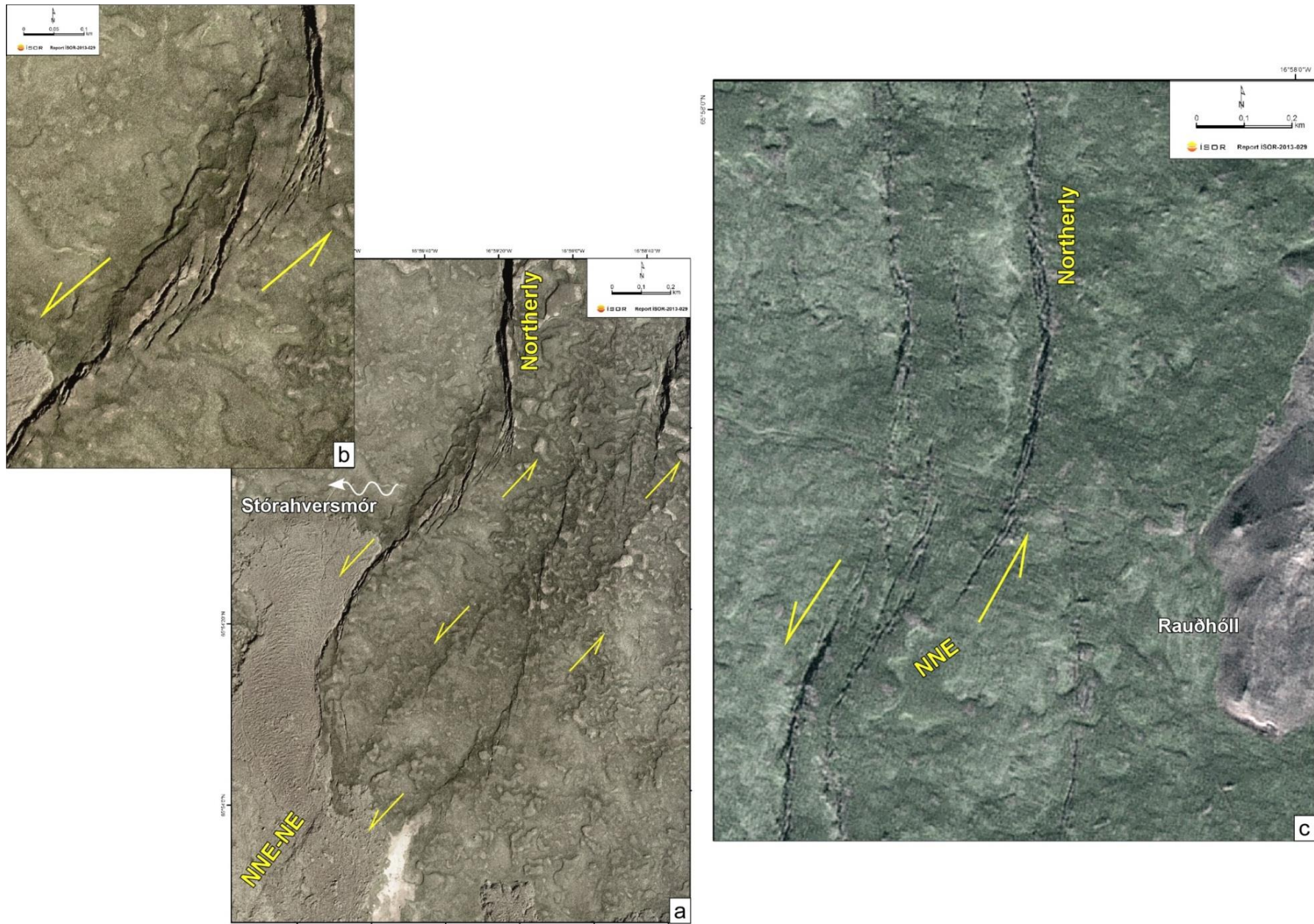


Figure 11. Examples of sinistral strike-slips based on right-stepping en échelon arrangement of open fractures at the surface. (a) Along the NNE / NE sets. (b) Close up of the westernmost fracture on (a). Both images are orthomaps. (c) Another example along the NNE set (image spot).

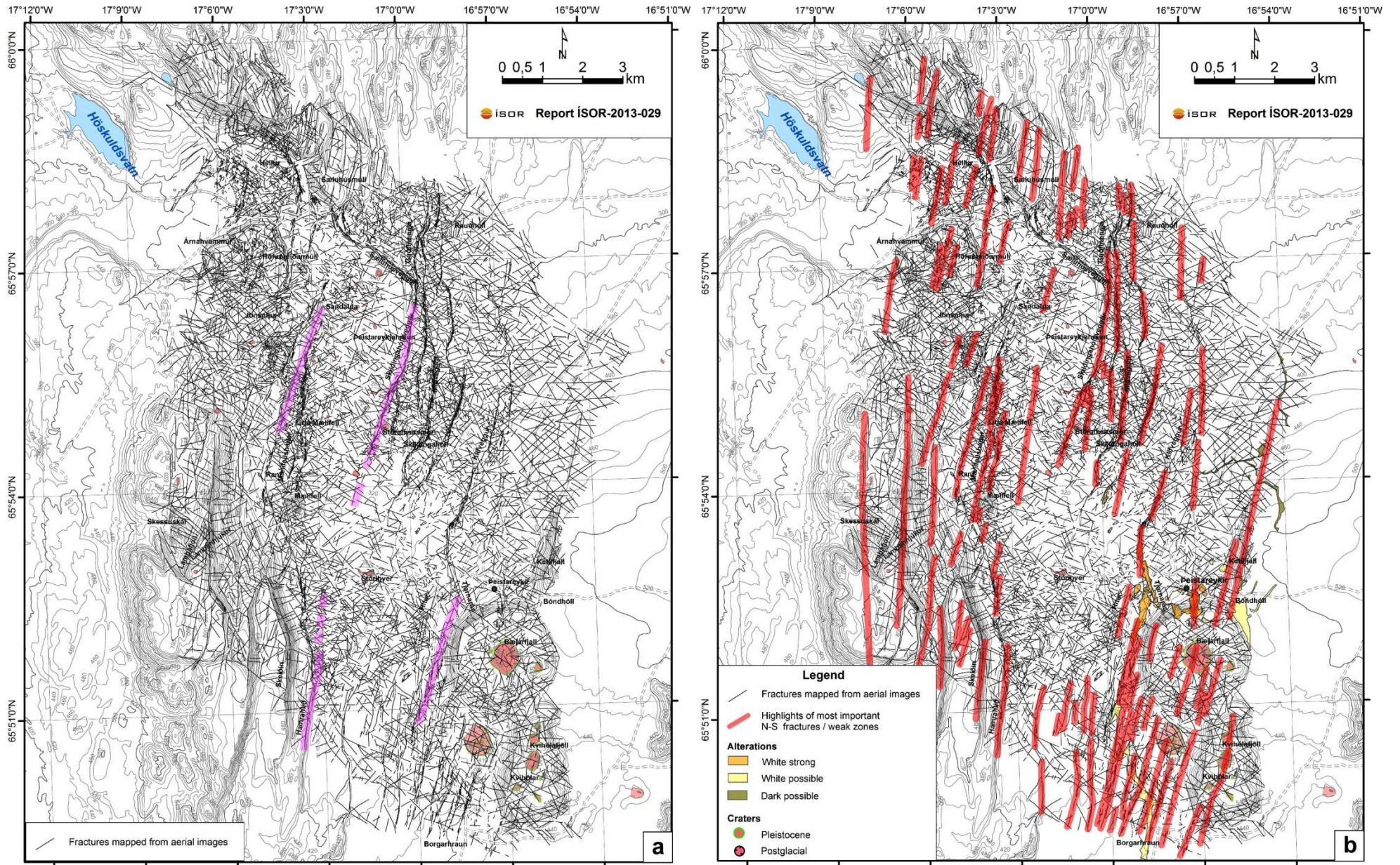


Figure 12. Highlights of rift-parallel northerly fractures / weak zones in Deistareykir fissure swarm. (a) Raw fractures from aerial imageries, where the approximate boundaries of two northerly grabens are also indicated in pink. (b) Interpretation of the most prominent northerly fractures.

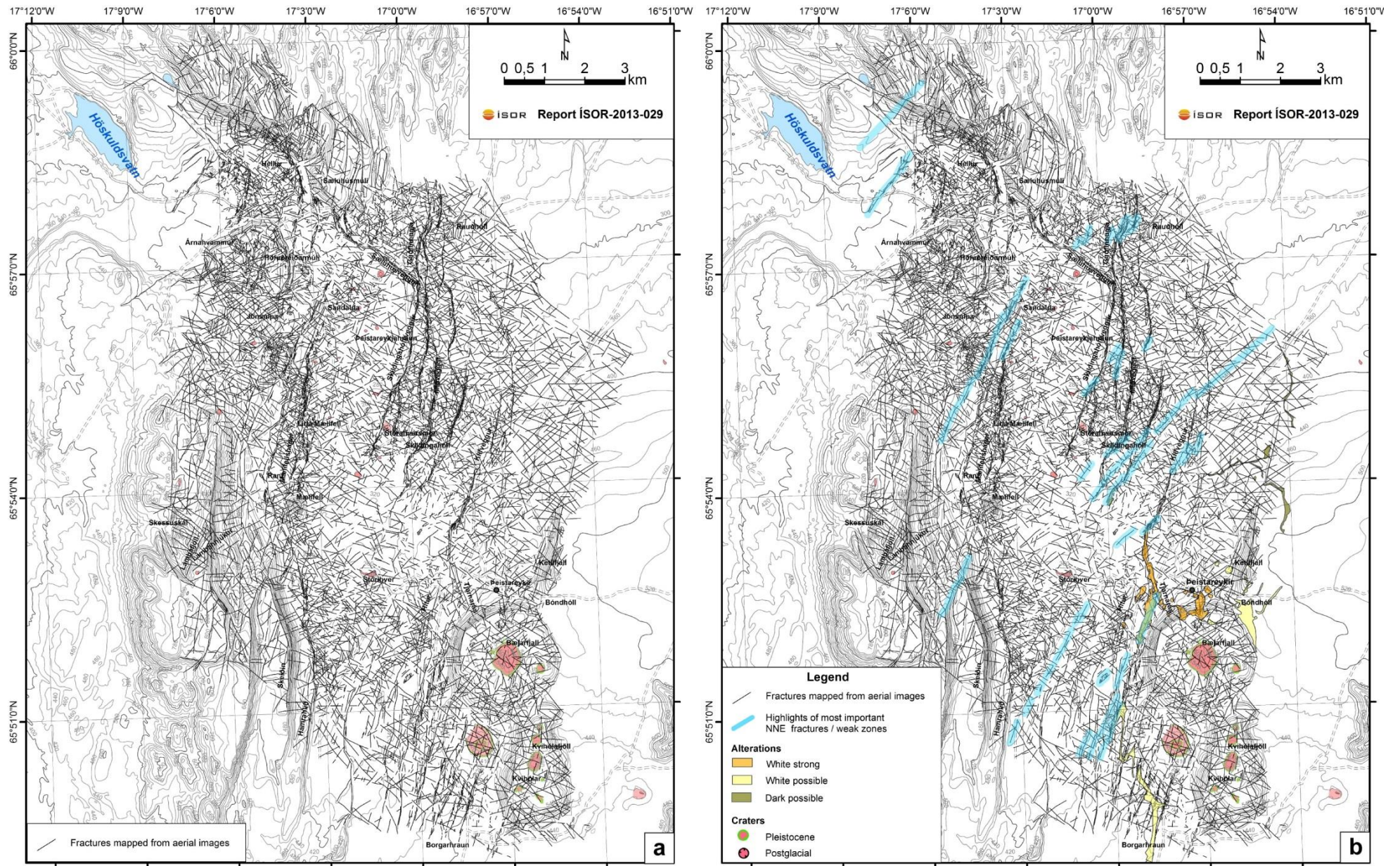


Figure 13. Highlights of NNE / NE fractures / weak zones. (a) Raw observations from aerial imageries. (b) Interpretation of the most prominent NNE / NE fractures, which show evidence of sinistral motion.

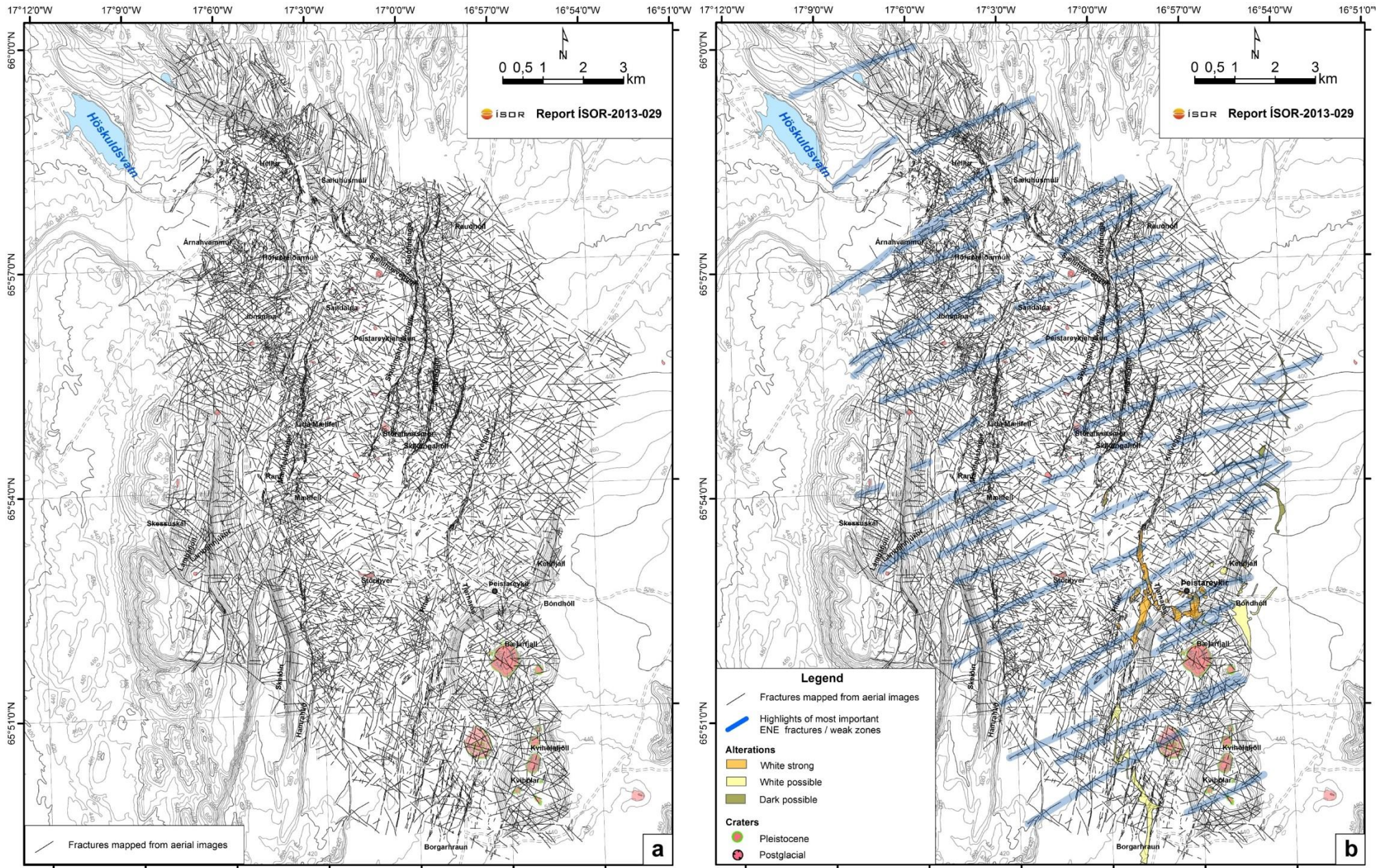


Figure 14. Highlights of ENE fractures / weak zones. (a) Raw observations from aerial imageries. (b) Interpretation of the most prominent ENE fractures.

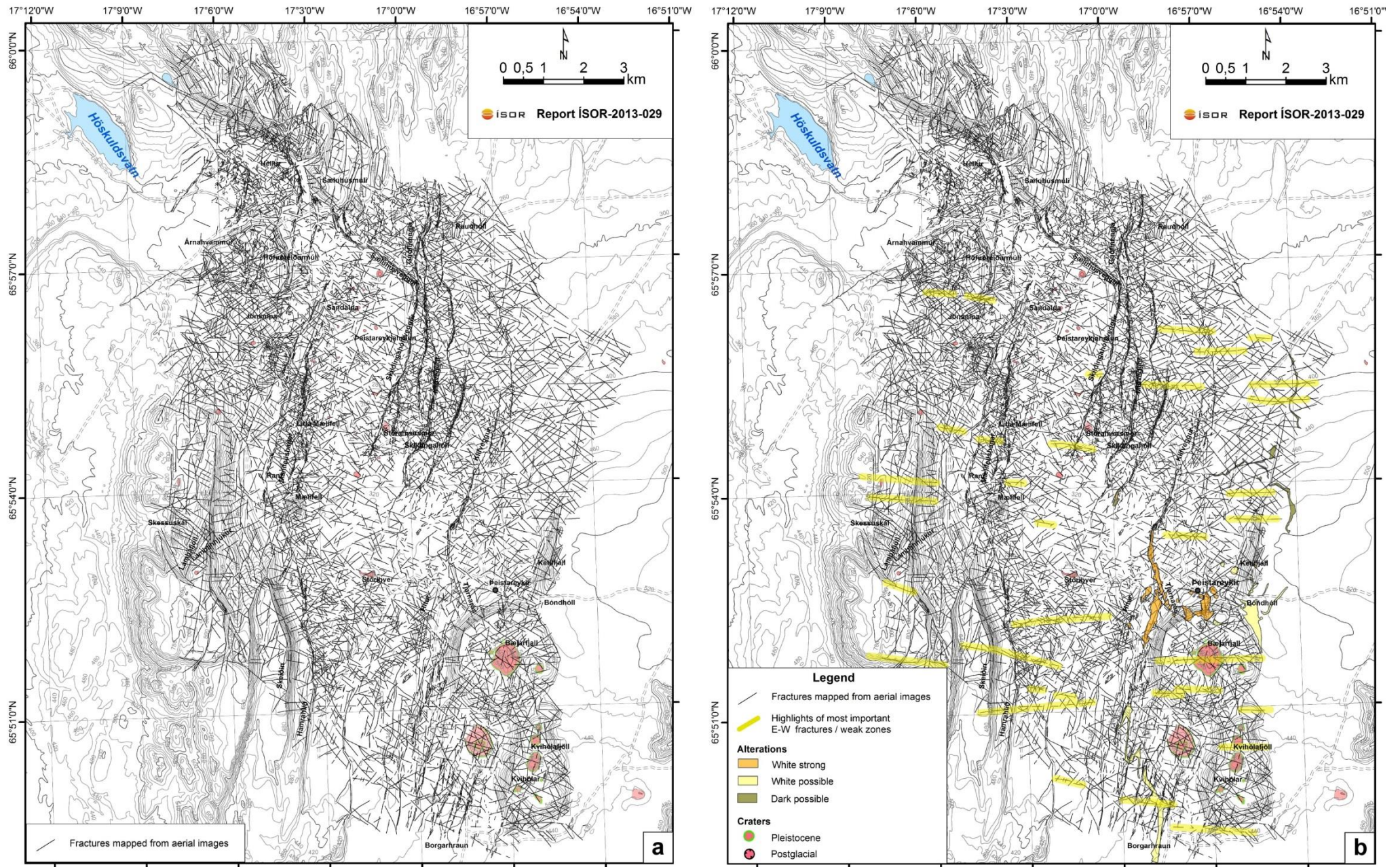


Figure 15. Highlights of E-W fractures / weak zones. (a) Raw observations from aerial imageries. (b) Interpretation of the most prominent E-W fractures.

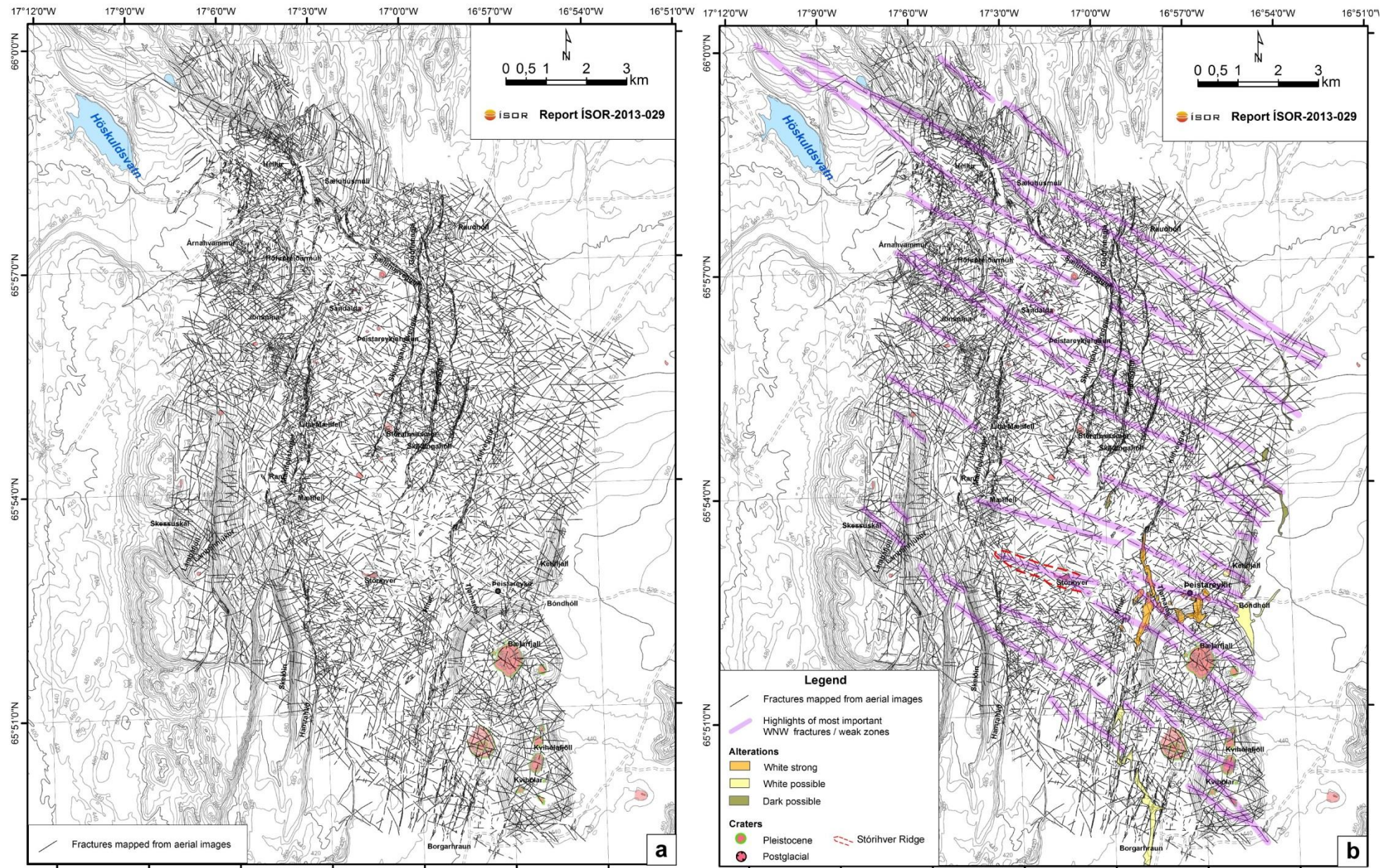


Figure 16. Highlights of WNW fractures / weak zones parallel to the transform zone of Tjörnes Fracture Zone. (a) Raw observations from aerial imageries. (b) Interpretation of the most prominent WNW fractures.

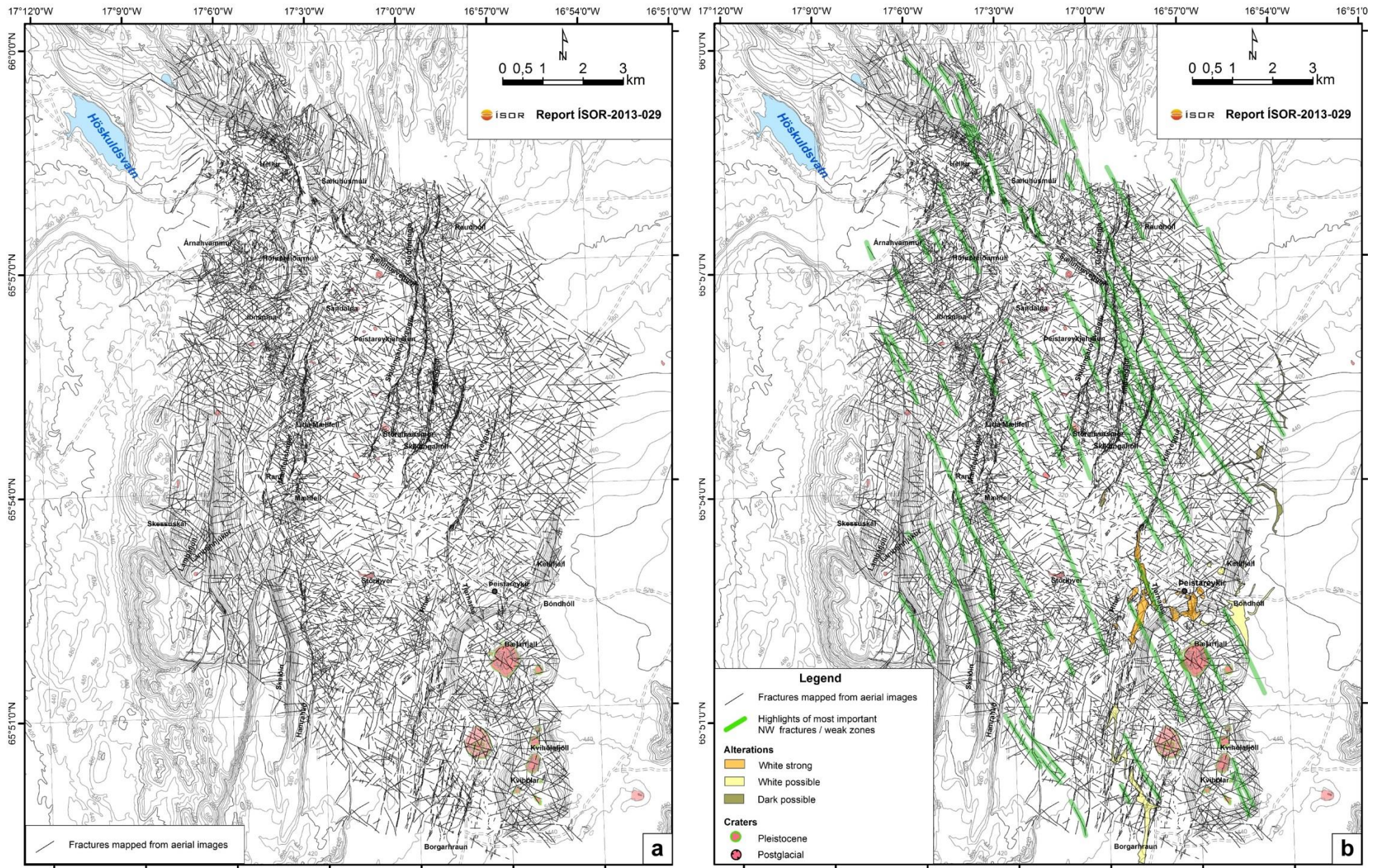


Figure 17. Highlights of NW fractures / weak zones. (a) Raw observations from aerial imageries. (b) Interpretation of the most prominent NW fractures.

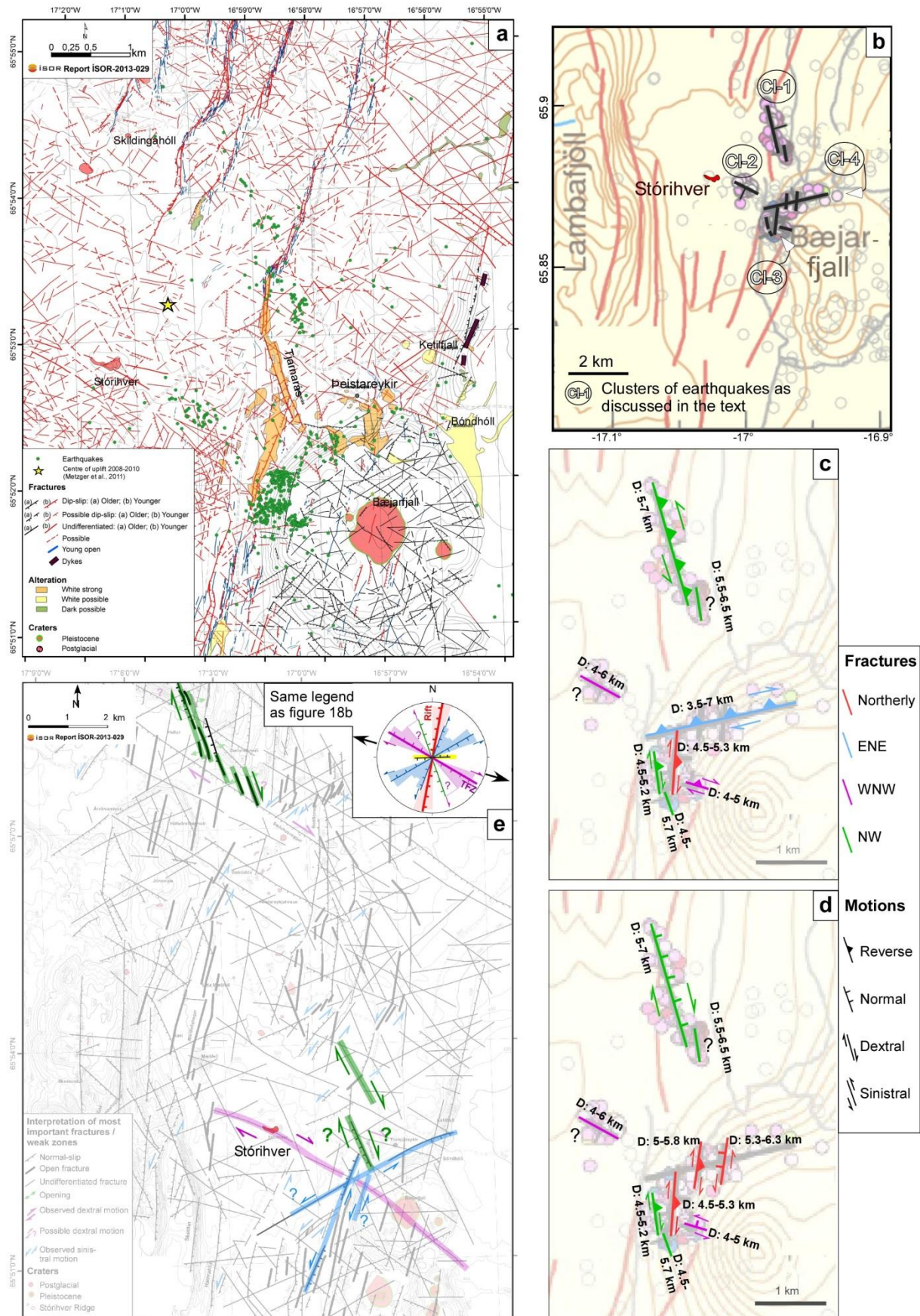
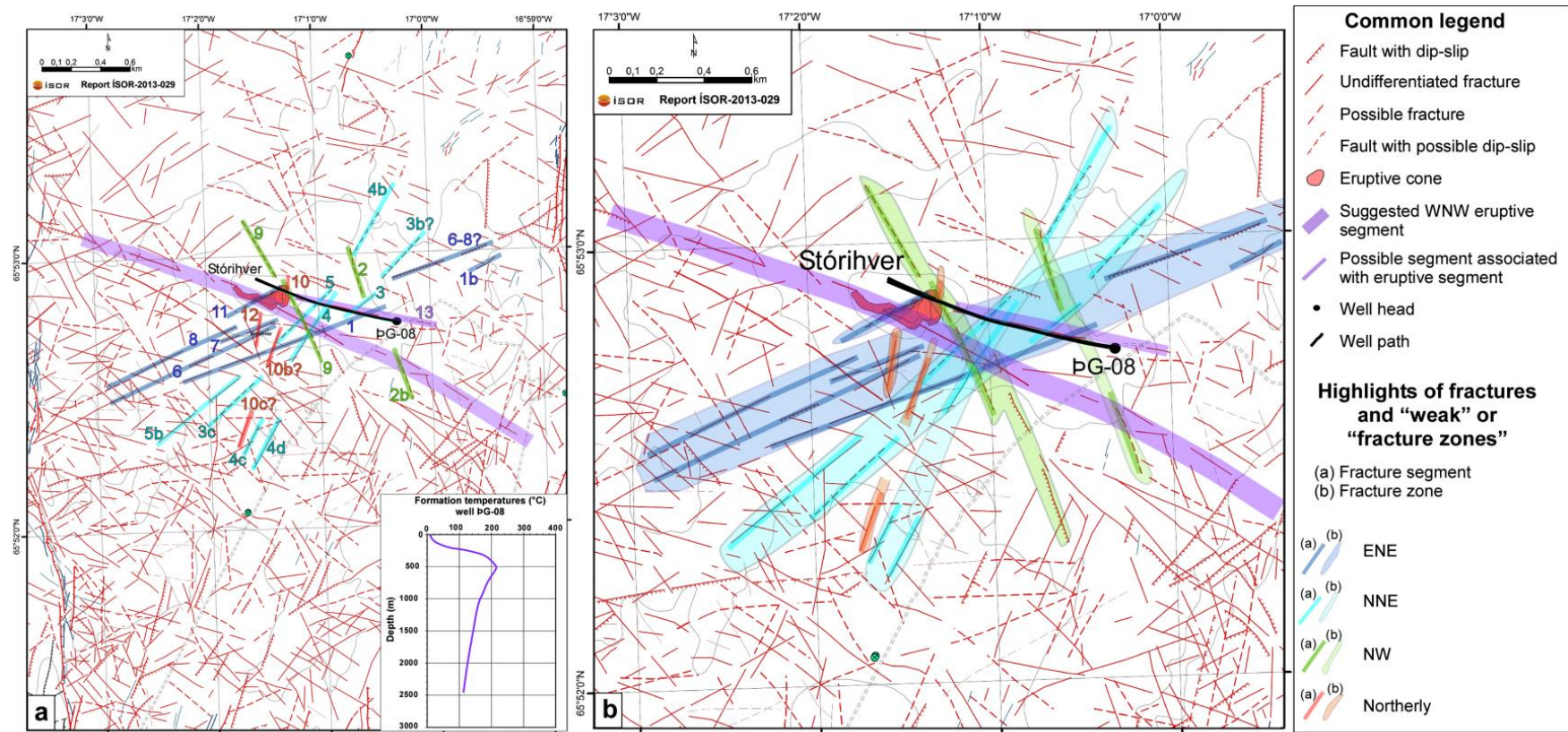
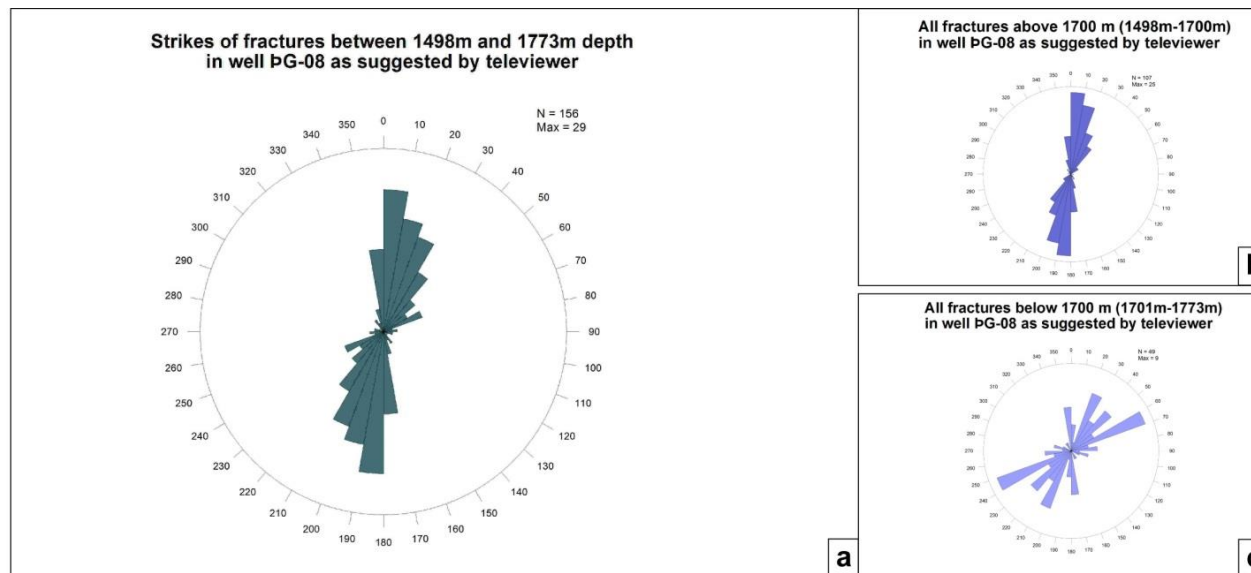


Figure 19. Correlation of our fracture pattern with relocated earthquakes (M -0.6 to 3.2) from 1993 to 2011. Earthquake data on figures 19a to 19 d are from Hjaltadóttir and Vogfjörð (2011), and the centre of uplift 2008–2010 on figure 19a is from Metzger et al. (2011). (a) Relocated earthquakes reported on our raw fracture map. (b) Four clusters of earthquakes and corresponding faults, along with two options (c) and (d) as to the motions along the faults (Hjaltadóttir and Vogfjörð (2011)). (e) Highlights of our fractures matching with relocated earthquakes and recall of our suggested strikes and motions (rose diagram).



Information on Well PG-08	Nr. allocated to individual segment on maps of Fig. 20	Fracture zones as suggested from this study, their distance from well head (dfwh), and equivalent in borehole depth			Feeders in well PG-08 projected at the surface	Drilled depths where feeders are reported	
		Strike of individual segment	Fractured zones formed by segments	Horizontal distance of fractures and fracture zones in terms of distance from well head (dfwh)			Drilled depth where fractures and fracture zones intersect the well
Inclined 30°. Drilled depth: 2430 m. Fractures intended to be intersected by drilling: N-S	1	N70°E	1	200 m	920 m		
	2	N 163°E	2	200 m	920 m		
	3	Possibly N52°E	3	~ 310 m	1133 m		
	4	N34°E (possibly)	4	~480m	1443 m		
	5	N44°E	5	550 m	1566 m		
	6	N65°E	6	580 m	1624 m	603 m, 605 m, 608 m	1680 m, 1683 m, 1688 m
	7	N65°E	7	630 m	1739 m	641 m and 655 m	1741 m and 1773 m
	8	N60°E	8	680 m	1848 m		
	9	N150°E	9	730 m (to 790 m?)	1969 m (to 2103 m?)	730 m	1970 m (to 2115 m?)
	10	N 11°E to N 20°E? (rift and sinistral strike-slip?)	10	760 m	2038 m		
	11	N60°E	11	820 m	2167 m	800 m and 830 m	2115 m, 2200 m
	12?	N08°E	12?	~ 940 m	2407 m	870 m	2260 m
	13	N 101°E	13	Parallel to the well between 120 m and 680 m; possibly intersecting the well?	758 m to 1848 m	950 m	2430 m

Figure 20. Brief correlation of our fractures with data from well PG-8. (a) Well path reported on our raw fracture map, with the highlights of the eruptive fissure and its tail at Stórihver, as well as other fracture sets intersecting the well. The formation temperature log is also inserted in the figure. (b) Zoom on the fractured “zones” comprising the suggested fracture segments intersecting the well. (c) Table showing the strikes and depths of our suggested fractures and correlation with the location of the feeders in the well. The colours on the table are the same as those used for the fractures on Fig. 20a and 20b. The pink letters highlight the depth of the main feeders in the well. See text for explanations.



Borehole depth	Equivalent of borehole depth as distance from well head	Zones of circulation loss and broken zones with apertures from 100-620 mm	Circulation loss	Strikes in broken zones
1575 m	543 m	121.69 mm	No	N10°
1581 m	546 m	291.08 mm	No	N178°
1665 m	593 m	205.10 mm	No	N23°
1670 m	596 m	306.48 mm	No	N08°
1683 m	603 m	240.43 mm	25 l/s	N21°
1686 m	605 m	328.54 mm	25 l/s?	N20°
1691 m	608 m	620.45 mm	25 l/s?	N168°
1720 m	624 m	278.25 mm	No	N21°
1724 m	626 m	131.45 mm	No	N06°
1751 m	641 m	43.96 mm	TOTAL	N41°
1773 m	655 m	00 (?) mm	TOTAL	N24°

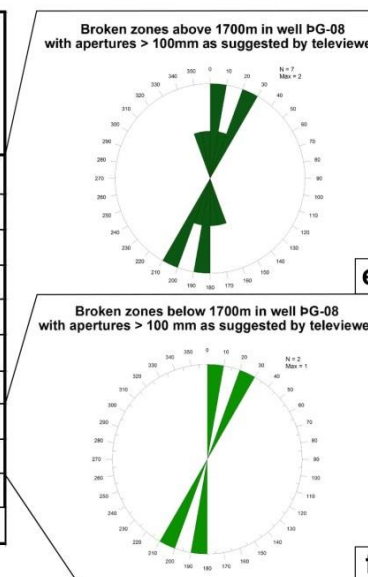
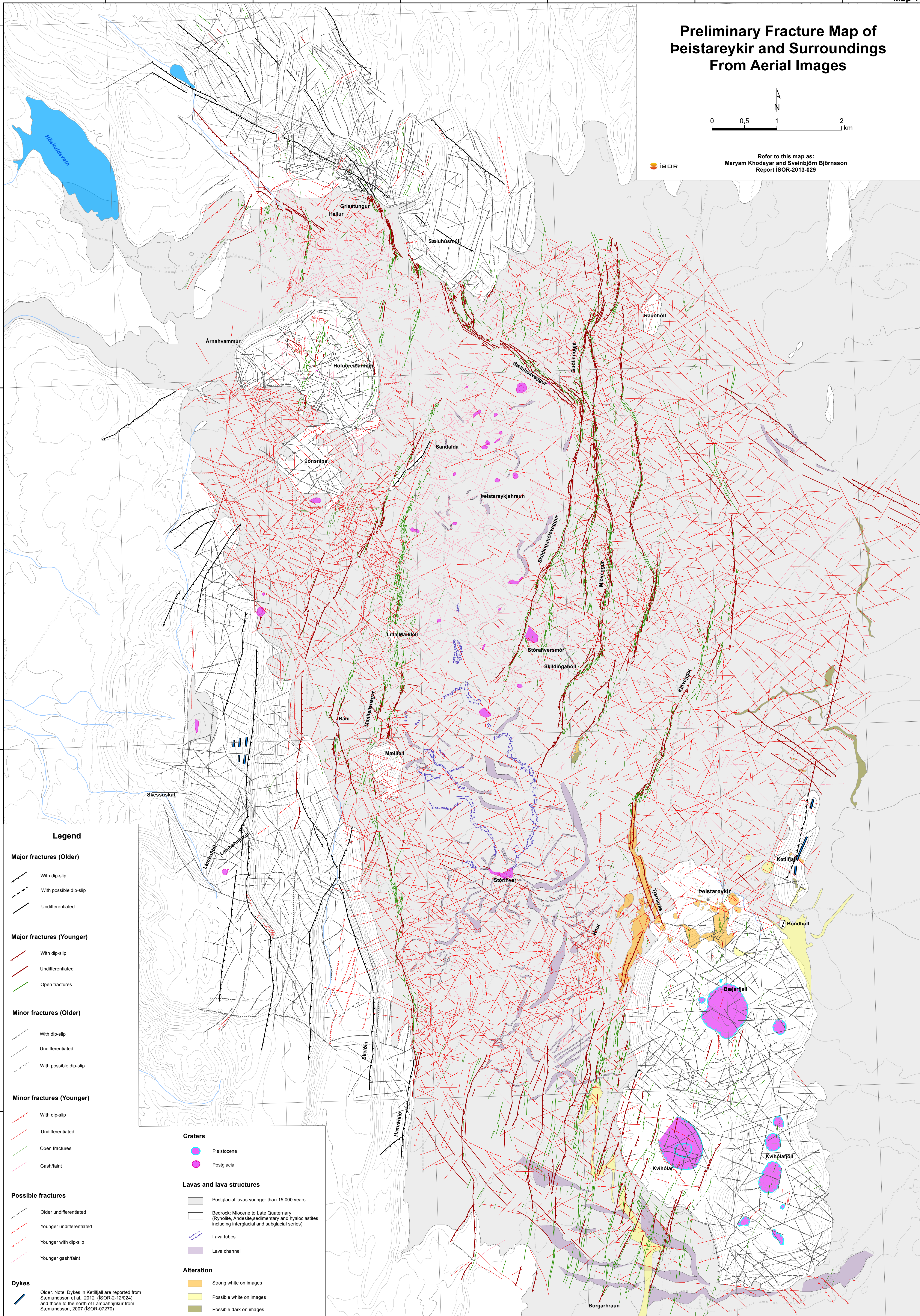


Figure 21. Fractures and widest broken zones from televiewer data along with circulation losses in well pG-8. (a) Strikes of all fractures. (b) and (c) Strikes of fractures above and below 1700 m drilled depth. (d) Correlation of the widest broken zones and the circulation losses at the same depths. The green color on the table highlights the largest circulation losses. (e) and (f) Strikes of the widest broken zones above and below 1700 m drilled depth.

Preliminary Fracture Map of Peistareykir and Surroundings From Aerial Images



Refer to this map as:
Maryam Khodayar and Sveinbjörn Björnsson
Report ISOR-2013-029



Legend

Major fractures (Older)

- With dip-slip
- With possible dip-slip
- Undifferentiated

Major fractures (Younger)

- With dip-slip
- Undifferentiated
- Open fractures

Minor fractures (Older)

- With dip-slip
- Undifferentiated
- With possible dip-slip

Minor fractures (Younger)

- With dip-slip
- Undifferentiated
- Open fractures
- Gash/faint

Possible fractures

- Older undifferentiated
- Younger undifferentiated
- Younger with dip-slip
- Younger gash/faint

Dykes

Older. Note: Dykes in Ketilfjall are reported from Sæmundsson et al., 2012 (ISOR-2-12/024), and those to the north of Lambahnjúkur from Sæmundsson, 2007 (ISOR-07270)

Craters

- Pleistocene
- Postglacial

Lavas and lava structures

- Postglacial lavas younger than 15,000 years
- Bedrock: Miocene to Late Quaternary (Rhyolite, Andesite, sedimentary and hyaloclastites including interglacial and subglacial series)
- Lava tubes
- Lava channel

Alteration

- Strong white on images
- Possible white on images
- Possible dark on images

Raw Lineament Map of Peistareykir and Surroundings From Aerial Images



Refer to this map as:
Maryam Khodayar and Sveinbjörn Björnsson
Report ISOR-2013-029



Legend

Mapped fractures

Undifferentiated

Craters

Pleistocene

Postglacial

66°0'0"N
65°57'0"N
65°54'0"N
65°51'0"N